ICMASET 2019

Proceeding:

International Conference on Modern Applied Science, Engineering and Technology Application (ICMASET 2019)

Bayview Beach Resort, Penang
25-26 September 2019

Published By:

GLOBAL ACADEMIC EXCELLENCE

eISBN 978-967-2245-16-2

eISBN: 978-967-2245-16-2

PUBLISHED BY:
GLOBAL ACADEMIC EXCELLENCE (M) SDN BHD
(1257579-U)
KELANTAN
MALAYSIA

International Conference on Modern Applied Sciences, Engineering and Technology Application 2019 (ICMASET 2019)
eISBN: 978-967-2245-16-2
25th - 26th September 2019,
Bayview Beach Resort, Penang, Malaysia

CONTENTS

International Conference on Modern Applied Sciences, Engineering and Technology Application 2019 (ICMASET 2019)
eISBN: 978-967-2245-16-2
25th - 26th September 2019,
Bayview Beach Resort, Penang, Malaysia

ANALYSIS OF LOW AND MEDIUM RISE REINFORCED CONCRETE (RC) BUILDINGS FOR LOW RISK EARTHQUAKE ZONE WITH EMPHASIS ON FRAMED STRUCTURE

Jeffrey C.L. CHIANG[1]
Zhi Xuan LIM[2]

[1]Faculty of Engineering & the Built Environment, SEGi University, Kota Damansara, Malaysia,
(E-mail: jeffreychiang@segi.edu.my)
[2] Faculty of Engineering & the Built Environment, SEGi University, Kota Damansara, Malaysia,
(Email: jonlzx85@gmail.com)

Abstract: *The majority of the Malaysian population do not associate Malaysia with earthquakes and seismic activity, hence, most of the reinforced concrete buildings had been designed in accordance to the previous British code of practice BS 8110, which has been phased out in UK since 2010. In Malaysia now, all RC building structures are to be designed to Eurocode 2 or EN1992. Although Malaysia is not located within any active seismic fault zone, some parts of the country do experience far-field earthquake effects from Sumatra Island, East of Indonesia. After having experienced the 2004 Aceh earthquake where some highrise building structures swayed substantially, the public raised some concerns about the integrity of the existing highrise buildings in Peninsular Malaysia to resist far-field earthquake tremors. In addition to Eurocode 2, Malaysia has also released the National Annex to Eurocode 8 or NA to MS EN1998, which is the European standards for seismic design now been adopted by Malaysia. Hence, the cost of construction according to seismic design may have a major economical impact on the Malaysia's local construction industry. In the interest of public safety and awareness, this research develops a detailed structural performance evaluation for typical RC low and medium rise buildings in Malaysia. At the same time, the difference in material resource usage between seismic design and non-seismic design is investigated. It is observed that the inter-storey drift ratio and the weight of steel reinforcement used in design is strongly influenced by the intensity of peak ground acceleration, a_{gR} and the corresponding structural behaviour factor, q.*

Keywords: *Peak ground acceleration, ductility, reinforced concrete, seismic, hazard*

Introduction

Earthquakes are one of the most devastating and unpredictable natural hazards which cause great loss of life and livelihood (Elnashai, 2008). Although Malaysia is located in the stable Sunda Shelf with low to medium seismic activity level, the seismic risk cannot be ignored (Manafizad, Pradhan and Abdullahi, 2016). It is inevitable to give considerable attention to the reactivation phenomenon of inactive faults, especially within the vicinity of 80km-long Bentong Fault. The epicenters were as close as 20 km to high population Kuala Lumpur, which a slight higher value of magnitude could have remarkable effects on seismic hazard of the region. In fact, historically, these earthquakes happened in rural area with low population and

have not yet inflicted any serious damage of buildings. However, due to the series of local origin earthquakes and increased of population in the rural area, government has urged the engineers to factor earthquake in development projects, especially for those on fault lines. The fact that, majority of the existing low- to mid-rise buildings in Malaysia including residential houses, schools, government offices and hospitals are suspected to have higher risk of collapsing compare to high-rise buildings. Since reinforced concrete (RC) requires less skilled labor and low maintenance cost, majority of these buildings are RC structures typically designed without provisions for earthquake-induced forces and are considered as weak to seismic loads. In the interest of public safety, this research develops a detailed structural performance evaluation for typical RC low and medium rise buildings in Malaysia. This paper also investigate the difference of steel reinforcement and concrete required when seismic provision is considered in reinforced concrete (RC) design of general hotel building.

Problem Statement

Although Malaysia is located in the stable Sunda Shelf with low to medium seismic activity level, the seismic risk cannot be ignored (Manafizad, Pradhan and Abdullahi, 2016). It is inevitable to give considerable attention to the reactivation phenomenon of inactive faults, especially within the vicinity of 80km-long Bentong Fault. The epicenters were as close as 20 km to high population Kuala Lumpur, which a slight higher value of magnitude could have remarkable effects on seismic hazard of the region. In fact, historically, these earthquakes happened in rural area with low population and have not yet inflicted any serious damage of buildings. However, due to the series of local origin earthquakes and increased of population in the rural area, government has urged the engineers to factor earthquake in development projects, especially for those on fault lines. The fact that, majority of the existing low- to mid-rise buildings in Malaysia including residential houses, schools, government offices and hospitals are suspected to have higher risk of collapsing compare to high-rise buildings. Since reinforced concrete (RC) requires less skilled labour and low maintenance cost, majority of these buildings are RC structures typically designed without provisions for earthquake-induced forces and are considered as weak to seismic loads.

Literature Review

European Code and National Annex Studies

Malaysia has adopted Eurocode (EN 1998-1) in the seismic design of reinforced concrete structures. The first edition of Malaysia National Annex to MS EN1998 Part 1: Design of Structures for Earthquake Resistance was drafted in 2017. Seismic hazard modelling of the region surrounding Malaysia with the methods mentioned in the previous chapters had been researched by the members in the authorship in order to produce the seismic hazard map and elastic model response spectrum for Peninsular Malaysia, Sarawak and Sabah (Lam, 2018). The key points from Eurocode 8 and Malaysia National Annex were studied in order to perform the analysis and design in this research.

Current Eurocode Provisions

Two fundamental requirements in seismic design is established in EN1998-1, which are as follows:

a) No-collapse requirement (Ultimate Limit State)
   In this requirement, it stated that for ordinary structures should be constructed and designed for a reference seismic action with 10% probability of exceedance in 50 years (475 year return period). In this case, this ensure that the building is able to withstand

the design seismic action without local or global collapse as the it is subjected a rare seismic event that can caused significant event.

b) Damage limitation requirement (Serviceability Limit State)
The requirement is to ensure that the building is designed to withstand a more frequent seismic action without damage. The limitation is related to the reduction of economic losses in terms of structural and non-structural in frequent earthquakes. No permanent deformation is alow to occur on the structure.

Hence, the two level seismic design requirements are actually depending on the probability of occurrence of the earthquake (JRC European Commission, 2012).

Seismic Parameters Studies Based on Eurocode 8 and Malaysian National Annex to Eurocode 8

In order to perform a detailed study and evaluation on the seismic performance of the low rise building, it is important to define the following seismic parameters based on the seismic code and National Annex of the respective country. The parameters are as follows:

1) Reference Peak Ground Acceleration
2) Building Importance factor
3) Behaviour Factor
4) Site Natural Period & Response Spectrum

Site Natural Period & Response Spectrum

In this study, only horizontal elastic response spectrum was considered in the analysis. The response spectrum was obtained by modal analysis. However, before proceeding to the analysis, several steps have to be taken in order to obtain the input parameters for the construction of soil response spectrum:

1) Obtain the Borehole report of the proposed site
2) Computation of site natural period, T_s from the borehole
3) Determine the ground type based on the ground classification scheme in accordance to site natural period, T_s
4) Select the Soil Factor, S, and corner periods T_B, T_C, T_D for the input into the response spectrum. Refer to Table 3.2 of Eurocode 8 (*BSI*, 2014).

However, in this study, no site work was done in order to obtain the borehole of the site. Hence, the site natural period, T_s was obtained based on the previous research works done by Dr Tsang (2016) to determine the suitable soil response spectrum that emphasis on the phenomenon of periodic ground shaking in Malaysia.

Analytical Procedure

In this paper, the modelling and design of an eight-storey RC building (based on Eurocode 2, Eurocode 8 and Malaysian National Annex to Eurocode 8) with different peak ground acceleration seismicity in Malaysia was carried out using Robot Structural Analysis Software.

Representative Building

Figure 1 shows an eight-storey regular hotel building that was modelled to represent the typical low and medium rise structures in Malaysia. For analyses, five building models were designed according to Eurocode 2 and Eurocode 8 with various level of reference peak ground acceleration, a_{gR} to mirror the Malaysian seismic hazard for ductility class low design (DCL) and ductility class moderate design (DCM). The layout, size of the building and load applied was repeated for each model. The building was assumed to be fixed at the base. Concrete

strength, beam and column size were maintained before the analysis. Modification will only be done if necessary. The detailing of steel reinforcement and concrete required was investigated and compared for the reinforced concrete (RC) design with and without seismic provision.

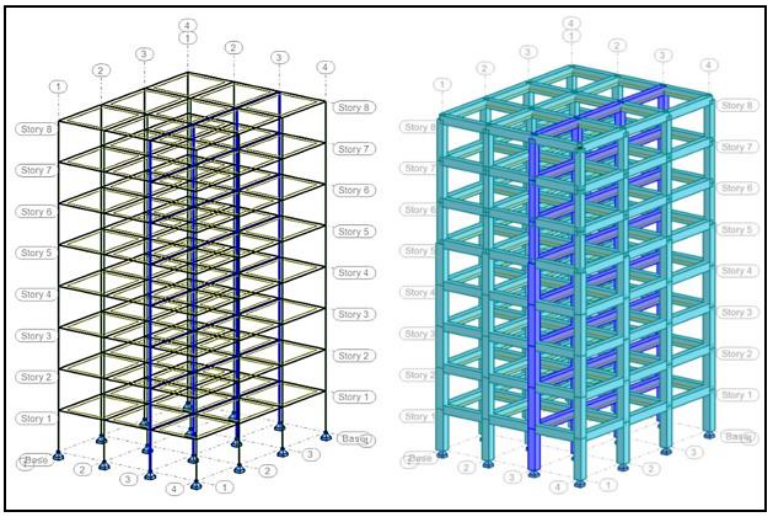

Figure 1. Model of an eight-storey regular building

Seismic Analysis of Various Case Studies

In this paper, the modal response spectrum analysis had been conducted on a typical structure frame of eight-storey RC building. For comparison, the similar building frame was used in five different case studies. In order to create case studies that reflect the seismic condition in Malaysia, several values of PGA were selected as reference peak ground acceleration, a_{gR} which is equal to 0.025g, 0.06g, 0.07g and 0.16g. All the values obtained from the Malaysia seismic hazard map. Table 1 depicts all the 5 cases in this study and their input parameters.

Table 1. Tabulation of input data for all five cases

Parameters	**Case 1**	**Case 2**	**Case 3**	**Case 4**	**Case 5**
Locations	Kuantan	Shah Alam	Kuala Lumpur		Lahad Datu
RPGA, a_{gR}	0.03g	0.06g	0.07g		0.16g
Importance factor, γ_I	1.2 (Building importance Class III)				
PGA, a_g	0.03g	0.07g	0.08g		0.19g
Soil Factor, S	1.35 (Soil Cass D, Type 1 Response Spectrum of Eurocode)				
PSA, a_{gS}	0.04g	0.97g	0.01g		0.25g

With the parameters in Table 1, each case study was classified based on the seismicity which are "very low seismicity", "low seismicity" and "low to moderate seismicity". All frames were design according to Eurocode 2 to represents current practice of RC design in Malaysia, however different seismic design approaches which is Low Ductility Class (DCL) or Moderate Ductility Class (DCM). Table 2 shows the design approaches adopted for each case.

Table 2. Design approaches for all five cases

Parameters	**Case 1**	**Case 2**	**Case 3**	**Case 4**	**Case 5**
Location	Kuantan	Shah Alam	Kuala Lumpur		Lahad Datu
PGA, a_g	0.03g<0.04g	0.07g<0.08g	0.08g>0.08g		0.19g
PSA, a_gS	0.04g<0.05g	0.97g<0.10g	0.01g>0.10g		0.25g
Seismicity	Very low	Low	Low-moderate		Low-moderate
Design Approaches	EC2	DCL	DCL	DCM	DCM
Behaviour factor, q	-	1.5	1.5	3.9	3.9

Modal Analysis

After computing the load cases on the model, modal analysis was performed in order to observe the vibration mode, natural period and the frequencies of building under wind load. For Case 1, since the seismic load was not applied in this case, the structural elements were assumed to be uncracked. Therefore, there was no stiffness reduction in this case. However, for other cases, the structural elements were assumed to be cracked. Therefore, the stiffness was reduced to one half. The modal responses are combined using the "Complete Quadratic Combination" (CQC) method assuming a modal damping of 5%. A total of 24 modes of vibration were considered in this analysis. After the analysis was done, the storey displacement and inter-storey drift ratio was observed for each cases and comparison was done.

Results and Discussion

Storey Displacement of Reinforced Concrete Structures

Based on Figure 2, it is observed that the maximum storey displacement of the RC structure has increased with the values of PGA. It can be said that more reinforcement is needed to maintain the stiffness of the structure when the values of PGA is high. The storey displacement of the structural system was obtained by modal response spectrum analysis based on the design response spectrum of each case. The displacement of the building depicts the deformation of the building when the earthquake happens. The structural performance of the structures was evaluated based on the interstorey drift ratio which is discussed in next subsection.

Interstorey Drift Ratio of Reinforced Concrete Structures

In this study, the interstorey drift ratio was used to estimate the structural performance of the building under seismic actions. According to EN 1998-1 (2004), limitation of interstorey drift is an additional damage limitation verification for RC design that is exposed to lateral forces in order to ensure the structure have sufficient stiffness for the functionality of the facilities. Hence, the limitation of interstorey drift controls the design approaches in most of the cases. The limitation of interstorey drift is based on the behaviour of non-structural materials that attached to the building structure(Soós, 2012). The behaviour of non-structural elements that take into account in this study is classified into brittle and ductile. Hence, by using interstorey drift limit above, the performance of the building in all cases was evaluated and compared. From figure 3, it can be concluded that the lateral drift of the structure in Case 1, Case 2, Case

3 and Case 4 is within the interstorey drift limit for building have brittle non-structural elements attached. This indicates that the structures have sufficient stiffness to resist the lateral force as the values of PGA in these cases are low.

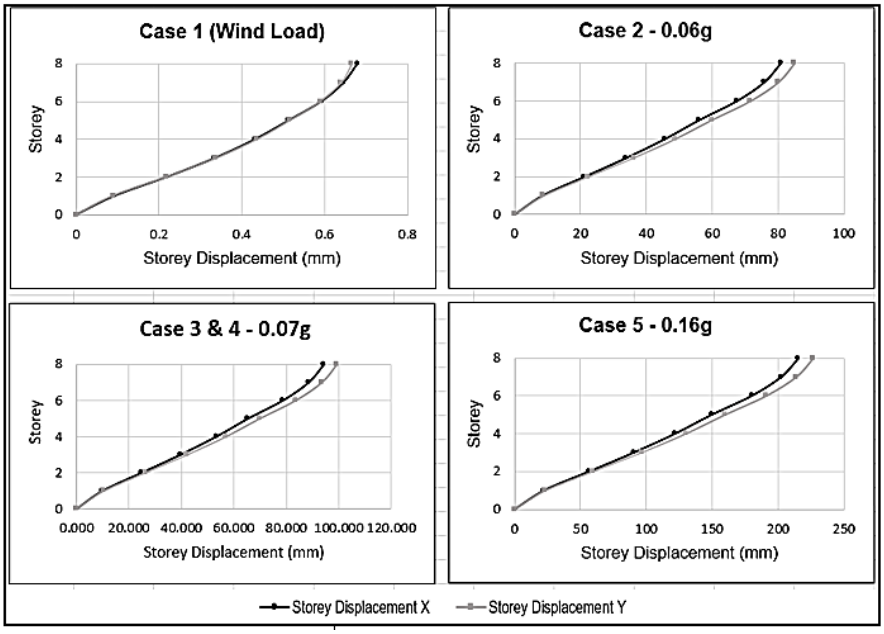

Figure 2. Storey displacements in centres of the masses in directions along X and Y

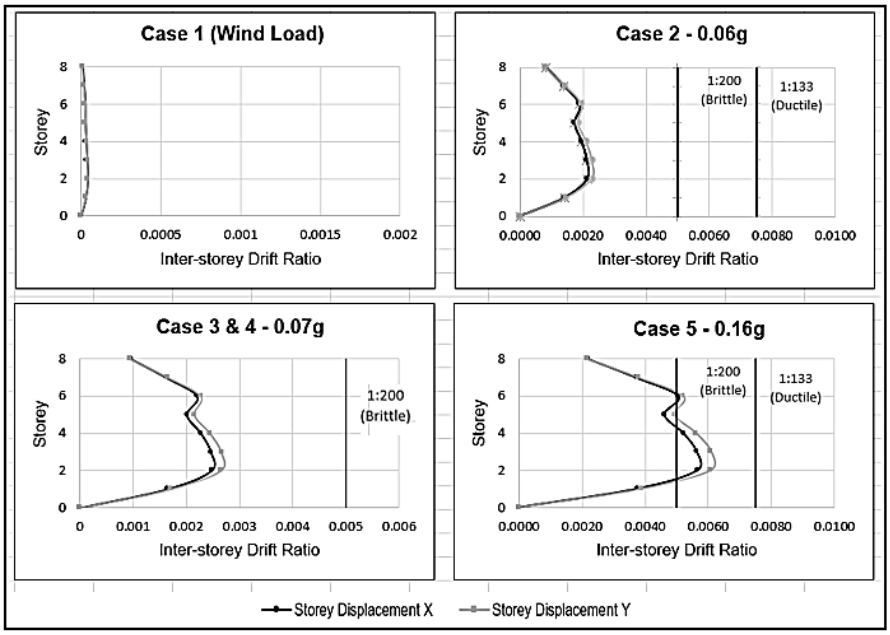

Figure 3. Interstorey drift ratio in directions along X and Y

However, for Case 5, the lateral drift of the structures has exceeded the interstorey drift limit for building have brittle non-structural elements attached. In other words, if there are brittle non-structural elements attached, it is necessary to increase the structure stiffness to reduce the interstorey drift. The high value of PGA has pushed the structures to drift over the boundary of the limit. In short, based on the performance evaluation, it clearly shows that

different level of ground shaking requires different seismic design approaches to ensure the designed structures have sufficient stiffness to withstand the seismic actions. The higher the values of PGA, the design of RC structure should be more ductile.

Material Used In Comparison for Typical Beam

Since it is difficult to establish an extra cost of the seismic design, material survey was done to investigate the extra weight of extra steel reinforcement needed in beam for seismic design. Without doubt, the amount of steel reinforcement provided in RC beam design is strongly associating with the bending moment and shear force from the load imposed on the structure. Longitudinal bar is responsible to resist the bending moment, while the transversal reinforcement is responsible to resist the shear.

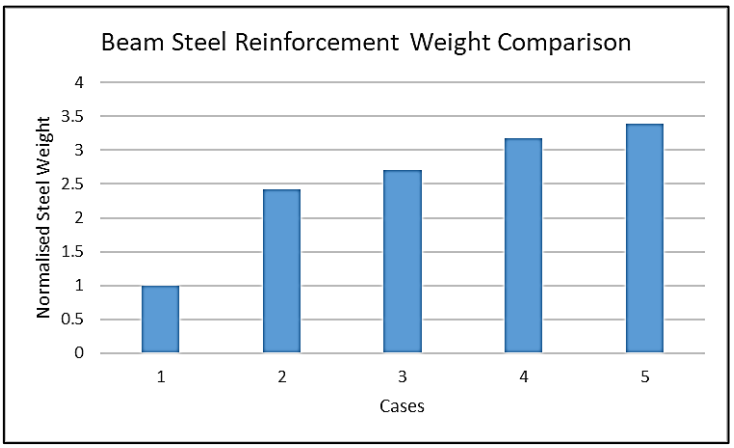

Figure 4. Normalised weight of steel reinforcement provided for a typical beam for all cases

Based on the graph, it can be observed that the total weight of steel reinforcement is increased in the range of 1 times to 2.5 times higher for frames design with seismic load. From the beam detailing in Figure 5.2, both the number of main bars and shear links increased with the values of PGA. This result can be related to the bending moment and shear force diagram of accidental limit state (ALS) shown in Chapter 4. In normal design that do not have seismic load case, for instance Case 1, ALS was not included in the design. Hence, this study has clearly shown that increment of total weight of steel reinforcement is affected by the increment of PGA values. Besides that, comparison between Case 3 and Case 4 shows that DCL is a better design approach that DCM, provided that the design acceleration ag or agS marginally exceed the threshold limit of low seismicity. Even though with a same value of PGA was applied in both case, DCL had resulted lower seismic demand and saving in the reinforcements. The main reason that contributed to this condition is due to the stringent requirement of detailing in DCM and also the minimum reinforcement requirements.

Material Used in Comparison for Typical Column

Similar to beam, normalised weight of steel reinforcement in Column 11 in all cases is shown in Figure 5. Based on the graph, it is observed that the weight of the steel reinforcement drastically increased in Case 4 and Case 5. This shows that the DCM approach requires more reinforcements compare to DCL. However, it is observed that the DCL design in both Case 2 and Case 3 requires almost same amount of reinforcement in normal RC design.

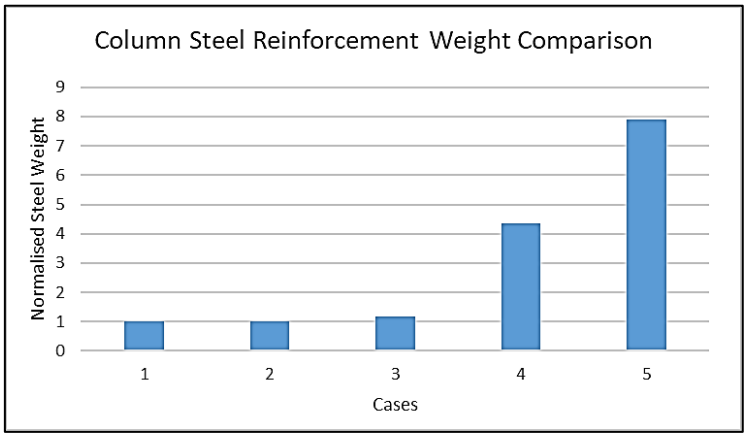

Figure 5. Normalised weight of steel provided for a typical column for all cases

As discussed in previous section, the interstorey drift ratio of the structure in Case 5 has exceed the limitation due to high value of PGA value. Thus, as a result, DCM design was adopted in this case in order to provide sufficient stiffness to the column by increasing the amount of the steel reinforcement. By this way, it can increase the ductility of the structure as steel is a very ductile material. The total weight of reinforcement for column is increased with the PGA values as higher shear force needed to be resisted.

On the other hand, the cross section of the column is also increased from 600 x 600 mm^2 to 700 x 700 mm^2 due to the section is overstressed if modification is not made. As a result, it shows that, the total volume of concrete is also influenced by the degree of PGA. The alternative to increase the concrete capacity is by increasing the concrete strength.

Conclusion

A total of five number of eight-storey RC building had been analysed with modal response spectrum analysis to evaluate the structural performance of the building. According to the classification of seismicity, the RC structures had been designed according to Eurocode 2 with and without seismic consideration to investigate the difference in material needed. Four different value of peak ground acceleration (PGA) had been considered in this research in order to cover the wide range of seismicity in Peninsular Malaysia, Sabah and Sarawak. As proposed by Eurocode 8, the value of behaviour factor, q for low class ductility (DCL) is 1.5 and 3.9 for moderate class ductility (DCM). All the frames had been evaluated with Modal Response Spectrum Analysis with software at different levels of PGA which are 0.03g, 0.06g, 0.07g and 0.16g. From the details presented in this paper, the following conclusion can be made:

1) In general, Malaysia is considered as low seismicity country. The PGA values for Peninsular Malaysia are ranged from 0.02g to 0.09g. Meanwhile, the PGA values for Sabah and Sarawak are ranged from 0.01g to 0.16g. The seismicity in Malaysia is classified into 3 zones which are very low seismicity zone, low seismicity zone and low to moderate seismicity zone. Hence, in this study, the reference peak ground acceleration, a_{gR} selected for the case studies have covered all the three seismic hazard zones for Malaysia.
2) The structural performance of the low to medium rise reinforced concrete (RC) structures was observed in terms inter-storey drift ratio. From modal response spectrum analysis, it had been proven that the inter-storey drift ratio of the structures increased with the intensity of PGA. For higher PGA, ductility design needed to be take into account in order to increase the stiffness of the structure and reduce the story drift.

3) In general, seismic zone with higher values of PGA will result in greater seismic demand which necessitate more reinforcement, higher concrete strength or greater section and longer storey drift.
4) Theoretically, using higher ductility class DCM will result lower seismic demand and saving in reinforcement. However, this study shows that, it may not apply where design PGA marginally exceeds the threshold of low seismicity definition. This is due to the stringent requirement of detailing in DCM compared to DCL and also minimum reinforcement requirements. It is suggested that DCL should be considered for the analysis and design in cases where appropriate.

Acknowledgments
The authors would like to acknowledge the contributions of members of the Technical Committee formed by The Institution of Engineers, Malaysia to draft the National Annex for the now published Malaysian Standards MS EN1998-1:2015 for design of earthquake resistant structures.

References
BS EN 1998-1 (2004). Eurocode 8: Design of Structures for Earthquake Resistance, BSI, London, 2004, 231p.
Elnashai, A. S. and Sarno, L. Di (2008) Fundamentals of Earthquake Engineering, John Wiley & Sons, Ltd.
Harith, N. S. H., Adnan, A. and Shoushtari, A. V (2014) 'Seismic Hazard Assessment of East Malaysia Region', 2(2008).
Irwan Adiyanto, M. and Majid, T. A. (2014) Seismic Design of Two Storey Reinforced Concrete Building In Malaysia With Low Class Ductility, Majid Journal of Engineering Science and Technology.
JRC European Commission (2012) 'Eurocode 8: Seismic Design of Buildings Worked examples', 1(2004).
Korkmaz, K. A. (2017) 'Structural Risk Assessment and Mitigation for Low- to Mid-Rise Residential Buildings in China', Frontiers in Built Environment. Frontiers, 3, p. 37.
Lam, Nelson et al. (2018) 'Earthquake Resistant Design of RC Buildings Based on the EC 8 M alaysia NA: From Loading Characterisation to RC Detailing', Proceedings of 2-Day Sym posium by The Institution of Engineers Malaysia, 18-19 Dec 2018.
Looi, D. T. W. et al. (2018) 'Seismic Hazard and Response Spectrum Modelling for Malaysia and Singapore', (July).
Manafizad, A. N., Pradhan, B. and Abdullahi, S. (2016) 'Estimation of Peak Ground Acceleration (PGA) for Peninsular Malaysia using geospatial approach', IOP Conference Series: Earth and Environmental Science, 37(1).
Shuib, M. K. et al. (2017) 'Active Faults In Peninsular Malaysia With Emphasis On Active Geomorphic Features Of Bukit Tinggi Region', Malaysian Journal Geosciences, 1(1), pp. 13–26.
Soós, M. and Vigh, L. G. (2012) On the Eurocode 8 limited damage criteria for non-structural elements – Analysis and requirements.
Tongkul, F. (2017) Active tectonics in Sabah-seismicity and active faults. Available at: https://gsm.org.my/products/702001-101721-PDF.pdf (Accessed: 23 October 2018).
Wang, Y. et al. (2017) 'The 2015 M w 6.0 Mt. Kinabalu earthquake: an infrequent fault rupture within the Crocker fault system of East Malaysia', Geoscience Letters, 4, p. 6.

Notation

a_{gR}	Referenced peak ground acceleration, m/s^2	K	Shear stiffness
a_g	Actual peak ground acceleration, m/s^2	v	Reduction factor
g	Gravitational acceleration, m/s^2	ϕ	Diameter in mm
S	Soil factor	f_{ck}	Concrete compressive strength
q	Behaviour factor	f_{yk}	Yield strength
q_o	Basic behavior factor		
γ_I	Importance factor	DCL	Ductility class low
T_s	Site natural period	DCM	Ductility class medium
G_k	Permanent action	DCH	Ductility class high
Q_k	Variable action	PGA	Peak ground acceleration
ψ_{2i}	Quasi-permanent value of the variable action	ULS	Ultimate limit State
T	Fundamental period	ALS	Accidental limit state
M	Storey mass		

International Conference on Modern Applied Sciences, Engineering and Technology Application 2019 (ICMASET 2019)
eISBN: 978-967-2245-16-2
25th - 26th September 2019,
Bayview Beach Resort, Penang, Malaysia

LAB SCALE STUDY ON INTEGRATED GSI FOR URBAN DRAINAGE SYSTEMS

Alias N.A.[1]
Mohd Fauzi, N.H.[2]
Yusuf, B.[3]
Meor Razali, M.M.F.[4]

[1,4] Faculty of Design and Architecture. Universiti Putra Malaysia (UPM), Malaysia, (E-mail: a_norazlina@upm.edu.my, meormohammad@upm.edu.my)
[2,3] Faculty of Engineering. Universiti Putra Malaysia (UPM), Malaysia, (Email: nisa@upm.edu.my)

Abstract: *Urbanization grows rapidly in Malaysia and has known to have several negative impacts. As development intensifies, water runs rapidly into rivers and less filters through the soil, contributes to the congestion of the stormwater drainage system that leads to the flash flood problem. Waste and pollution transported by stormwater also posed environmental problems, thus several open drain systems were introduced to improve it. However, some of those open drainage systems contributes to more pollutions and worsened the quality of life of the urban dwellers in Malaysia. Several approaches with different concepts have been developed, including the Best Management Practices (BMPs), Low Impact Development (LID), Water Sensitive Urban Design (WSUD), Sustainable Urban Drainage Systems (SUDS), Innovative Stormwater Management and the Green Stormwater Infrastructure (GSI). This paper proposed the potential system that gives minimal impact to the environment while improving the water filtration and flood control system in the urban areas. The GSI system can effectively address water environment issues caused by traditional stormwater drainage systems. Research focuses on the development and application of an integrated GSI storage used in urban areas adapted to flood risk with the used of bio-composite material. A lab scale system was developed to study the performance of bio-composite materials and the design of inner storage as an infiltrator as runoff decelerator. Results showed that the used of rice husk and coconut fibre as an infiltrator improved the quality of rainwater. The integrated GSI that was designed to have an inner storage also elongates the surface runoff time. It is expected that the proposed design of eco-friendly integrated storage for drainage system could prevent ponding and at the same time the contaminated flow will be filtrated by the embedded bio-composite materials before entering the water bodies.*
Keywords: *Integrated Storage, Stormwater, Bio-composite, Urban Drainage*

Introduction

In the event of urban rainstorm, less surface runoff infiltrated into the soil due to the reduction of permeable area. It contributes to the congestion of the stormwater drainage system due to increased paved areas which in turn causing severe flash flood incidences (Aminuddin, et al. 2003). The excessive of sediment that built up in the drain also reduced its storage capacity and lead to ponding and flooding (Alex, et. al, 2001). The changes in land use have become apparent and the degree of soil imperviousness increases especially in developing countries had led to the increased of stormwater volume (Kundzewicz, et al., 2007). As development intensifies, so more water runs rapidly into rivers and less filters through the soil. This sealing of the ground can and does lead to localised flooding and water pollution and will only get worse as our climate changes. As a result, flooding events are commonplace in many cities of the world. An increase in stormwater runoff becomes the source of water pollution as stormwater transports

large quantities of contaminants to receiving waters in many countries including Malaysia (Lee, et al., 2007). Boller (1997) stated that the pollutants from streets and roofs carried by stormwater was the major contributor in surface water pollution. The pollution transported also posed quantity and quality problems that affect the public health and the environment. Due to decreasing pervious areas and deterioration of water quality in stormwater runoff, a possible drainage system for stormwater runoff were designed; however, some of those open drainage systems contributes to more polluted river and worsened the quality of life of the urban community in Malaysia. Ashantha, et. al (2005) concluded that the more develop the country is, the poorer the water quality they have.

Worldwide, most of the countries that were affected by flood disasters have taken an integrated action to overcome or at least minimize the impacts of flood by establishing flood risk management. Several approaches with different concepts have been developed. These include the Best Management Practices (BMPs), Low Impact Development (LID), Water Sensitive Urban Design (WSUD), Sustainable Urban Drainage Systems (SUDS), Innovative Stormwater Management and the Green Stormwater Infrastructure (GSI). The GSI system can effectively address water environment issues caused by traditional stormwater drainage systems, thus this study focuses on the development and application of an integrated GSI used in urban design adapted to flood risk. Flood event also results in relevant economic and social costs because of building and personal property damage (Ntelekos et al., 2010). Therefore, stormwater runoff must be properly managed to prevent floods and to protect water resources and public health. Each Urban Drainage System functioning with different efficiency depending on its design and hydraulics parameters. Failure of any systems implemented may undermine its performance and cause an excessive amount of stormwater runoff that results in urban flooding. This research aims to develop and propose a lab scale integrated model or system with the intention to overcome or at least minimize the impact of flood in impervious areas.

This paper proposes a new tangible product of GSI to reduce the flood risk and improve the stormwater quality while maintaining the greeneries in the developed or urbanized areas. The improvement of the eco-friendly drainage system will be able to contribute to the Sustainable Development Goals (SDGs) which include a dedicated goal on resilient infrastructure. SDG #9 is a call to “Build resilient infrastructure, promote sustainable industrialization and foster innovation”. A prototype of Eco-friendly Integrated GSI was produced. Proposed integrated GSI considered a storage in order to control potential pollutants before discharging water to a storm drain. Laboratory scale study were conducted in order to analyse the performance of the proposed system. Collected water through the infiltration system were tested for its quality. It is expected that the proposed design of Integrated GSI Storage block could increase the flow velocity to prevent ponding that leads to urban flooding and at the same time polluted runoff will be filtrated by the bio-composite materials embedded to the designed block before entering the water bodies. It is hope that the system with its potential can be used and implemented in urban areas that facing the flood problems and will contribute in knowledge information on the most suitable or the best flood risk management in urban areas.

The Integrated GSI

The Brick

A new approach is needed in which drainage allows storage and keeps the runoff water on site longer, prevents pollution and eventually the collected water can be used for a range of non-potable uses. Thus the Integrated GSI mortar brick is designed to have an inner opening acting as storage to elongate the surface runoff time. It is also expected that the proposed design of

eco-friendly integrated storage for drainage system could prevent ponding while at the same time the contaminated flow will be filtrated by the embedded bio-composite materials before entering the water bodies. A single Integrated GSI brick is design to have 200 m x 75 mm x 80 mm (length x width x thick) with 30 mm x 30 mm x 80mm (length x width x thick) opening in the middle. The opening section is to be filled with selected bio-composite materials and to reduce brick individual's weight. The brick was casted in halved for easy handling with average weight of 1.85 kg. Two halved bricks were assembled in which the opening sections are facing together as in Figure 1 making the brick's overall dimension of 200 m x 150 mm x 80 mm with an opening of 60 mm x 30 mm x 80mm in the middle. The schematic diagram of the brick is as in Figure 2.

Figure 1 : The Integrated GSI Brick

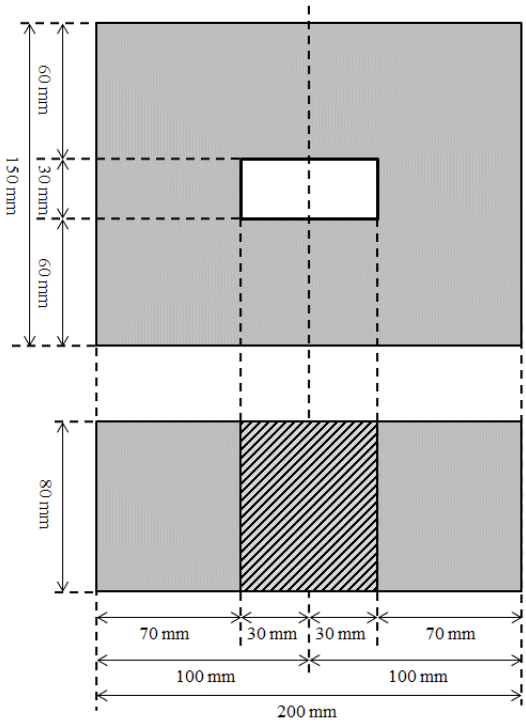

Figure 2 : The Integrated GSI Brick Schematic Diagram

Selection of Bio-Composite Materials

A non-wood bio-composite material used in this study are the type of straw and fruit fibers such as rice husk and coconut fiber. Those dry rice husk and coconut fiber were placed and compacted in the opening section. The main purpose of using these biological wastes is to infiltrate small particles and at the same time increase the quality of rainwater before entering

the water bodies. The second intention is to promote the vegetation growth where this Integrated GSI being implemented. Figure 3 shows the types of bio-composite materials used in this study.

a) Rice Husk **b) Coconut Fiber**

Figure 3 : Bio-composite materials used

Lab Scale Study

About 106 bricks were casted using a steel mould as in Figure 4 below. Those bricks were then arranged in a specifically designed rainfall simulator. The rainfall simulator has a rectangular basin sized 2000 mm by 1000 mm in length and width respectively. Figure 5 shows the bricks arrangement in the rainfall simulator basin. The rainfall simulator's tank was filled up with the earlier collected rainwater. Rainwater was collected at Hydraulic Laboratory, Faculty of Engineering University Putra Malaysia representing the existent quality of rainwater in selected study area. More than 100 liters rainwater was collected on a rainy day to fill up the Rainfall Simulator tank. The rainwater stored in the tank was then pumped and flowed into sprinkler systems imitating actual rainfall at required intensity. The rainwater samples were first tested for it quality as a benchmark and then compared to the rainwater that have been stored and filtered by the bio-composite materials embedded in the proposed Integrated GSI.

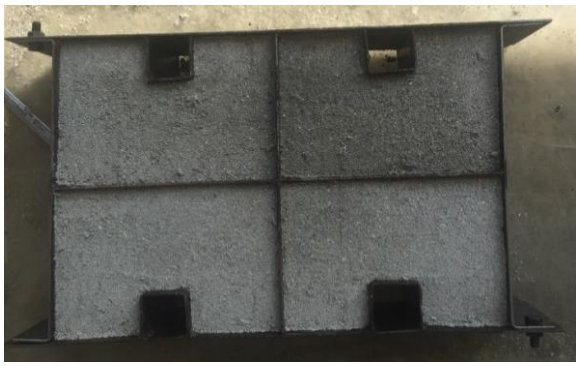

Figure 4 : Steel Mould Used To Case Integrated GSI

Figure 5 : Integrated GSI Arrangement Inside The Rainfall Simulator

The storm water quantity or peak discharge (Q_{peak}) of the location was estimated using Rational Method as in Equation 1:

$$Q_{peak} = \frac{CIA}{360} \quad \text{…Equation 1}$$

where Q_{peak} is the peak discharge in m^3/s, C is a dimensionless runoff coefficient, I is rainfall intensity in mm/hr, A is catchment area in hectares and the conversion factor is taken as 360.

The peak discharges at 2, 5 and 10 years of ARIs were calculated and imposed representing maximum peak discharge of a rainstorm event. For lab scale study, the selected urban area was scaled down to 1m length x 7m width equivalent to 0.0007 hectares. The discharges imposed while conducting three sets of experiments are tabulated as in Table 1.

Table 1: Peak Discharge For Duration Of 5 Minute For The Experimental Areas Of 7m^2

ARI	Duration (min)	Rainfall Intensity, *I* (mm/hr)	Runoff coefficient, *C*	Area (Hectares)	Peak Discharge, Q_{peak} (m^3/s)
2	5	250	0.95	0.0007	0.00046
5	5	280	0.95	0.0007	0.00052
10	5	320	0.95	0.0007	0.00059

Runoff samples quality were tested to assess the effectiveness of the chosen bio-composite material as filter substance. The collected rainwater (non-filtered) was tested for its quality and compared with the one that flowed and infiltrated (filtered) through the eco-friendly bio-composite materials. Both results were then compared with national water index parameter by Department of Environmental, Malaysia. The compared parameters include pH, biochemical oxygen demand (BOD), chemical oxygen demand (COD), turbidity, total dissolve solid (TDS), total suspended solid (TSS) and ammonia nitrogen test in determining the runoff quality.

Results And Discussion

Integrated GSI Performance

As mentioned earlier, the experiments were conducted on an Integrated GSI bricks with two different types of bio-composite materials (rice husk and coconut fibre) and on Integrated GSI bricks without the bio-composite material referred as a benchmark test. The first test conducted was the benchmark test as shown in Figure 6. The second and third tests conducted were on the integrated GSI systems that filled with rice husk and coconut fibre respectively as shown in Figure 7(a) and Figure 7(b). Each test were run for three times at different discharge imposed.

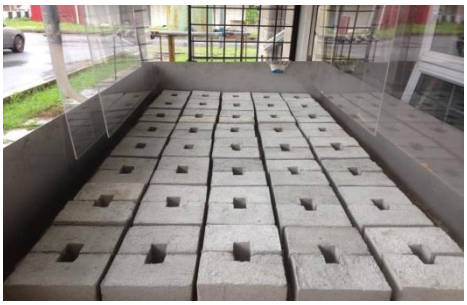

Figure 6 : Integrated GSI System Without Bio-Composite Material As The Benchmark Test

A) Rice Husk

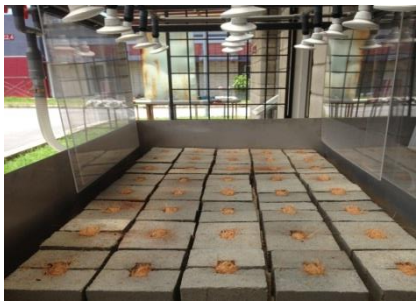

B) Coconut Fiber

Figure 7 : Integrated GSI System With Bio-Composite Materials.

Tests were run with initial discharge of 0.00046 m^3/s for 2 ARI, 0.00052 m^3/s for 5 ARI and 0.00059 m^3/s for 10 ARI. The discharges were recorded at every 30 second and after five minutes the rainfall simulator valve was shut down to stop the rainfall. The discharges were continuously recorded until there is no outflow.

For the first run, initial discharge of 0.00046m^3/s for 2 ARI was imposed. The graph line in Figure 8 shows that the peak discharge for benchmark test (Integrated GSI without bio-composite material) was 0.00064m^3/s and recorded at the 300s. While the peak discharge for Integrated GSI system with the rice husks and coconut fibre were 0.00061m^3/s at time 300s and 0.00062m^3/s at time 270s respectively. Both rice husk and coconut fibre were found to reduce the peak discharge by 5% and 3% respectively in comparison with the benchmark test. It can be seen from Figure 9, the surface runoff volume recorded in the Integrated GSI system with both Rice Husk and Coconut Fibre are lesser compared to the system without bio-composite material. This indicates that both materials have an ability to store the rainwater and reduced the amount of surface runoff while avoid the ponding condition. At simulation time 300s, the surface runoff volume for a system using rice husk as infiltrator was greater than the benchmark as the opening area was filled up by water. Comparing between two types of bio-composite materials, system with the coconut fibre has lower surface runoff volume than the system with rice husk. This may be due to the coconut fibre that is more porous compared to the rice husk which was able to store more rainwater.

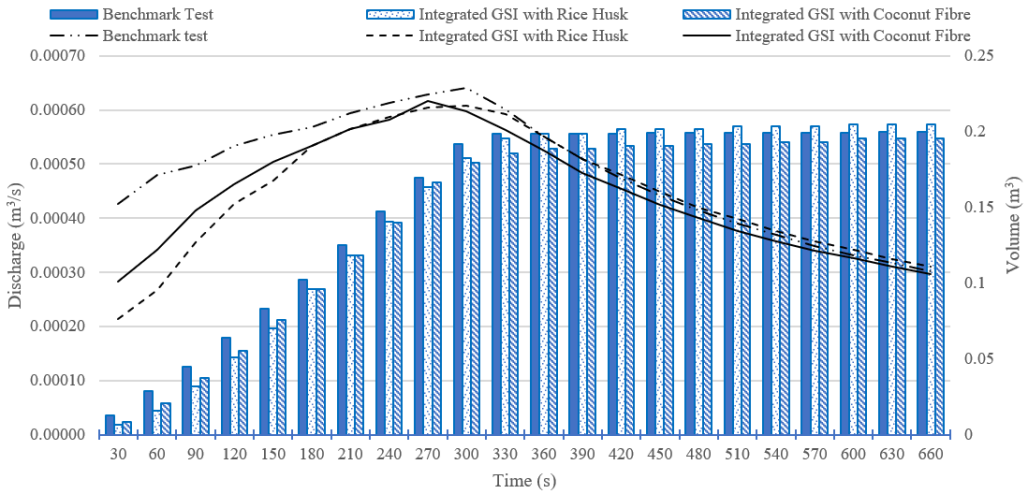

Figure 8 : Comparison on Peak Discharge at 2 ARI

On the second run, initial discharge of 0.00052m^3/s for 5 ARI was imposed and the results are as illustrated by line graph in Figure 10 below. The benchmark peak discharge recorded was 0.00071m^3/s at 4 minute and 30 second, while peak discharges for both systems with rice husk and coconut fibre were 0.00068 m^3/s and 0.00066m^3/s respectively at 5-minute duration. This shows that both materials able to reduce the discharge to be lower than the benchmark discharge by 4% and 7%. Figure 9 also shows that at first 5-minute, rice husk and coconut fibre have lower runoff volume compared to system without filter substance. This indicate that both material able to store water while reducing the discharge resulting in delaying the peak discharge time. Rice husk and coconut fibre managed to store about 2% and 3% more water in the inner storage. Coconut fibre was found better in detaining water due to its absorbent characteristic.

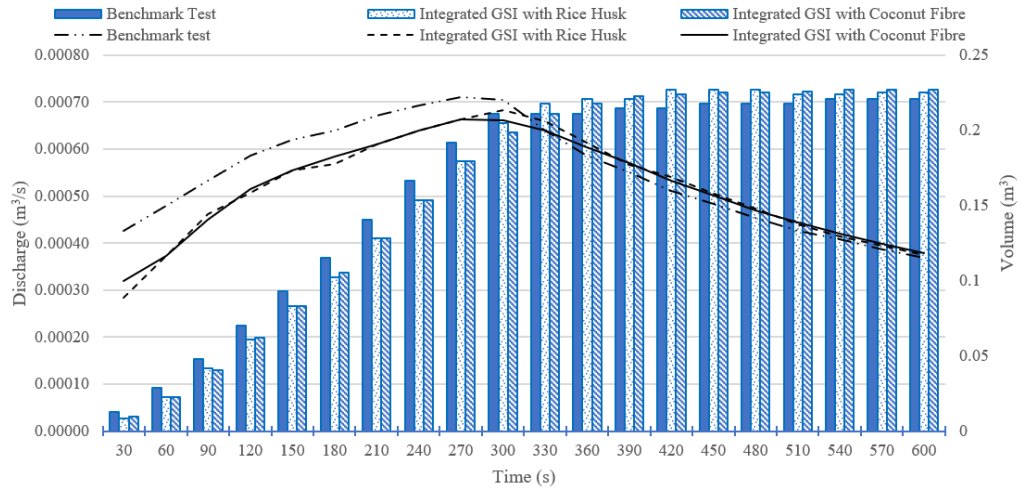

Figure 9 : Comparison on Peak Discharge at 5 ARI

In the third run, initial discharge was set at 0.00059m^3/s (10 ARI). The comparison on discharge and runoff volume detained is shown in Figure 10. From the graph, it shows that the peak discharge at 270s for benchmark test is 0.00081^3/s. The peak discharges for Integrated GSI for both rice husk and coconut fibre are 0.00079m^3/s and 0.00077m^3/s respectively and recorded at 300s. The trend lines show that both rice husk and coconut fibre peak discharges

are lower than the benchmark. Both rice husk and coconut fibre were able to reduce the peak discharge by 2.5% and 5% respectively. It also shows that the used of bio-composite materials were able to attenuate of peak flows by elongating the peak discharge time.

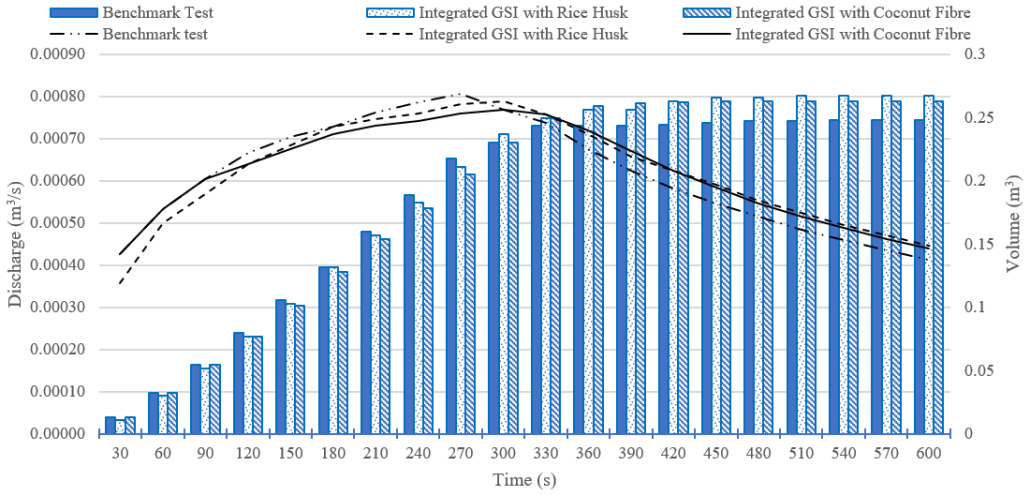

Figure 10 : Comparison on Peak Discharge at 10 ARI

Figure 11 shows the storage capacity between rice husk and coconut fibre. There is significant difference in storage capacity between Rice Husk and Coconut Fibre in the first run of experiment where only 0.00046m^3/s discharge imposed. Rice husk was also found good in storing rainwater in the first and third run while coconut fibre was performing better in the second run where 0.00052m^3/s discharge was imposed. The ability of Rice Husk in storing rainwater was increasing as the discharge increase.

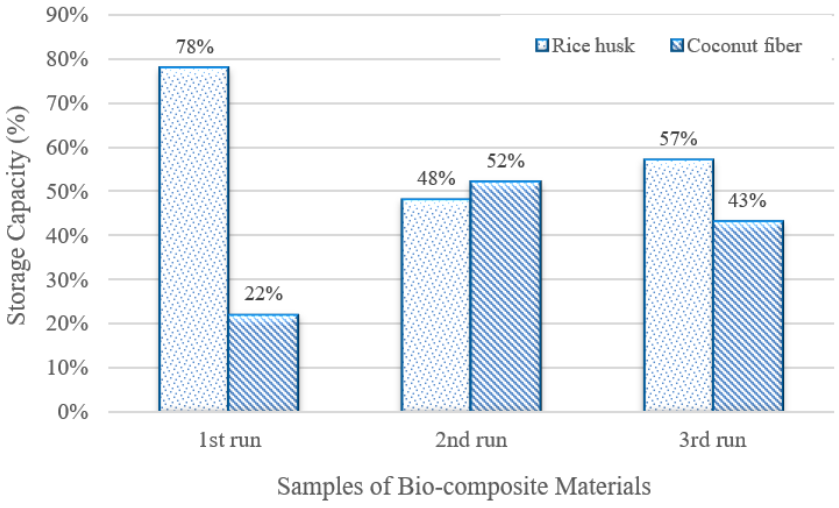

Figure 11 : Bio-composite Material Storage Capacity

Water Quality

Determination of Water Quality

The rainwater quality results obtained by conducting pH, turbidity, bio-chemical oxygen demand (BOD), chemical oxygen demand (COD), total dissolve solid (TDS), total suspended solid (TSS) and total ammonia nitrogen. The results from collected rainwater that was directly tested for its quality was taken as reference or benchmark results and was compared with the

quality of rainwater filtered by rice husk and coconut fibre through the Integrated GSI brick. Table 2 below show the water quality results.

Table 2 : Water Quality Results of Rainwater Sample

Parameter	Benchmark	Bio-composite materials	
		Rice Husk	Coconut Fiber
pH	4.38	9.84	9.73
Turbidity (NTU)	1.96	2.11	2.95
Total Suspended Solid (mg/l)	20	5	5
Total Dissolve Solid (mg/l)	70	40	45
Total Ammonia Nitrogen (mg/l)	0.02	0.0114	0.0114
BOD (mg/l)	2.7	1.3	1.8
COD (mg/l)	32	16	16

Based on the Table 2 above, rainwater filtered through both eco-friendly materials gave lower readings in most tested parameters than the benchmark test. There are significance differences in values recorded except for the Turbidity and pH. Generally, it indicates that those materials are capable and performing well in filtering the rainwater. A huge reduction on Total Suspended Solid and Total Dissolve Solid of filtered rainwater compared to the non-filtered rainwater. This shows that both bio-composite materials are efficient in retaining the solid residue in rainwater. For the reading of Total Ammonia Nitrogen, it was low since the amount of ammonia in rainwater is very minimum. The implementation of both rice husk and coconut fibre however reduced the reading to 40%. The pH of filtered water is slightly over the standard requirement which is 5-9 and become more alkaline. This high value of 9.84 and 9.73 may be due to the bio-composite material that influenced the pH value when mixed with water. The standard water quality for Total Suspended Solid (TSS) parameter range is 25mg/l. The Total Suspended Solid recorded for benchmark sample was 20mg/l while both rice husk and coconut fibre recorded 5mg/l. Both materials were found better in retaining 75% of suspended solid in the rainwater sample. Again, based on the experiments conducted to check the Total Suspended Solid, the benchmark test reading was 70mg/l whereas both rice husk and coconut fibre recorded 40mg/l and 45mg/l respectively. For turbidity, both filtered rainwaters recorded higher values than the benchmark. The benchmark was 1.96NTU while turbidity test on rainwater filtered by rice husk and coconut fibre recorded 2.11NTU and 2.95NTU respectively. Both dusty bio-composite materials contributed to the increased in turbidity readings. Results could be more accurate if those materials were washed and cleaned from impurities before experiments were conducted.

Conclusion

Based on the results obtained from the laboratory experimental works, it shows that the proposed Integrated GSI with the used of rice husk and coconut fibre embedded in the opening area as bio-composite materials are efficient in reducing the stormwater discharge and delay the discharge reaches its peak by storing the surface runoff.

In the first run where 0.00046 m^3/s peak discharge was imposed, Integrated GSI brick with rice husk and coconut fibre were found able to reduce 5% and 3% of the peak discharge respectively. Again, comparing the peak discharges for both systems with and without the bio-

composite materials, the rice husk and coconut fibre were able to record peak discharges 4% and 7% lesser 0.00052 m^3/s in the second run. However, when 0.00059 m^3/s discharge imposed in the third run, the rice husk and coconut fibre were able to reduce the peak discharge by only 2.5% and 5% respectively. It can be concluded that the opening storage integrated at the centre able to reduce the amount of peak discharges.

In terms of the water storing performance, rice husk embedded in the Integrated GSI system was able to store additional 3% of water while the coconut fibre detained water lesser than system without bio-composite material in the first run. This may be due to the characteristic of coconut fibre which is slow in absorbing water. In the second run, the rice husk and coconut fibre were able to store additional 2% and 3% respectively. It was recorded that about 8% and 6% extra water were stored by both Integrated GSI system with rice husk and coconut fibre respectively in the third run of the experiment. The results showed that the storage capacity increased inversely with the discharge imposed.

In terms of runoff quality, it shows that rice husk and coconut fibre materials can also be used in preliminary stage of water treatment in which the bio-composite materials were capable to act as runoff filtering system. The runoff was quite acidic with pH of 4.38 was recorded. The pH values were 9.84 and 9.73 after filtrated by the rice husk and coconut fibre. The sudden increment in pH might be influenced by those bio-composite materials themselves. The quality of runoff that infiltrated through the bio-composite material was improved. Both rice husk and coconut fibre materials were able to reduce the Total Dissolve Solid (TDS) by 43%, Total Suspended Solid (TSS) by 75% and Total Ammonia Nitrogen by 4.3%. The Biochemical Oxygen Demand (BOD) was reduced by 53% and 33% with the used of rice husk and coconut fibre respectively. For the Chemical Oxygen Demand, both rice husk and coconut fibre materials reduced its reading to 50%. From results obtained, the bio-composite materials such as rice husk and coconut fibre were found capable in improving the rainwater quality.

It can be concluded that the research objectives have been achieved where the proposed Integrated GSI is able to reduce and delay the peak discharge by introducing an inner opening in the design. From experiments conducted it also shows that the opening has good capability in storing rainwater. In terms of water quality, the proposed Integrated GSI was also performing well in increasing the rainwater quality before releasing it into the water bodies. However, it is suggested that this research to be extended with the used of various types of bio-composite materials; for example, Kenaf, the sugar cane husk, betel husk etc. in order to study their performance in storing and filtrating the runoff.

Acknowledgments

The first author thanks the Universiti Putra Malaysia (UPM), for providing financial support under the Putra Research Grant (GP-IPM9661700). The second author acknowledges the support from Civil Engineering Department for assistance with field data collections and laboratory works.

References

Ahmad, Z., & Kothyari, U.C. (2001). Time-line cubic spline interpolation scheme for solution of advection equation. *Journal of Computational Fluids*. 30,737-752.

Alcrudo, F., & García-Navarro, P. (1993). A high-resolution Godunov-type scheme in finite volumes for the 2D shallow water equations. *International Journal of Numerical Method In Fluids*. 16 (6), 489-505.

Alex, S., Andrew, S. K., Robert, Y. G. A. and Michael G. F. (2001). A Novel Integrated System for Stormwater Management. 4th International Conference of Innovative Technologies in Urban Drainage, France. 23-25 June. 433-440.

Allen, D.,Olive, V., Arthur, S.,and Haynes, H. 2015 Urban Sediment Transport through an Established Vegetated Swale: Long Term Treatment Efficiencies and Deposition. *Journal Water*, 7, 1046-1067.

Aminuddin, A. G., Nor Azizi, Z., Lariyah M. S. and Rozi, A. (2003). Bio-ecological drainage system (BIOECODS) for water quantity and quality control. *International Journal of River Basin Management*. 237-251.

Argue, J.R. and Pezzaniti, D. 2007, 'Towards Sustainability of Waterways in Urbanising Catchments', Proceedings of NOVATECH, France 279-286.

Ashantha, G., Gilbert, D, Ginn, S., and Thomas, E. (2005). Understand The Role of Land Use in Urban Stormwater Quality Management. *Journal of Environmental Management*. 74: 1-2.

Ashantha, G., Gilbert, D, Ginn, S., and Thomas, E. (2005). Understand The Role of Land Use in Urban Stormwater Quality Management. *Journal of Environmental Management*. 74: 1-2.

Boller, M. (1997). Tracking Heavy Metals Reveals Sustainability Deficits of Urban Drainage Systems. *Journal of Water, Science and Technology*. 35: 77-87.

Butler, D. and Parkinson,J.,1997. Towards Sustainable Urban Drainage. Water Science and Technology. (35). 53-63.

Fletcher, T.D., Hatt, B.E. and Deletic, A., 2006. Integrated Treatment and Recycling of Rtormwater: A Review of Australian Practice. *Journal of Environmental Management* 79 (1), 102-113.

Garden Design Access on 22/2/ 12.39pm http://www.brand-garden.com/garden/water-drainage/

Jones, A., Stovin, V., Guymer, I., Gaskell, P., and Maltby, L. 2008. Modelling Temporal Variations in the Sediment Concentrations in Highway Runoff. In: Proceedings from the 11th International Conference on Urban Drainage, Edinburgh, UK

Kundzewicz, Z.W., Mata, L.J., Arnell, N., Döll, P., Kabat, P., Jiménez, B., Miller, K., Oki, T., Şen, Z. And Shiklomanov,I. 2007. Freshwater resources and their management. Climate Change 2007: Impacts, Adaptation and Vulnerability. The Fourth Assessment Report of the Intergovernmental Panel on Climate Change

Lee, H., Swamikannub, X., Radulescub, D., Kimc, S.,and Stenstrom, M.K., 2007. Design of Stormwater Monitoring Programs. Water Research 41 (18), 4186-4196.

Leroy, M., Portet-Koltalo, F., Legras, M., Lederf, F., Moncond, F., Polaert, I., and Marcotte, S., Performance of Vegetated Swales for Improving Road Runoff Quality in a Moderate Traffic Urban Area. *Journal of Science of The Total Environment*. 566–567 (2016) 113–121

Ntelekos, A.A., Oppenheimer, M., Smith, J.A. and Miller, A.J., 2010. Urbanization, Climate Change and Flood Policy in the United States. Climatic Change 103 (3-4), 597-616.

Raymond S. and Marian P.,1999. Permeable Paving Stone System. Report presented for SF Concrete Technology Inc.

Roinas, G., 2014. Fate and Behavior of Pollutants in a Vegetated Pond System for Road Runoff. Research Article Clean Soil Air Water

Saeedi, M., Daneshvar, S., and Karbassi, A.R. 2004. Role of Riverine Sediment and Particulate Matter in Adsorption of Heavy Metals. *International Journal of Environmental Science Technology*. 1(2):135–140

Siriwardene, N.R., Deletic, A., and Fletcher,T.D. 2007. Clogging of Stormwater Gravel Infiltration Systems and Filters: Insights from a Laboratory Study. Water Res. 41(7), 1433–1440

International Conference on Modern Applied Sciences, Engineering and Technology Application 2019 (ICMASET 2019)
eISBN: 978-967-2245-16-2
25th - 26th September 2019,
Bayview Beach Resort, Penang, Malaysia

EFFECT OF PROCESSING SPEED ON MICROSTRUCTURE AND COLOUR PROPERTIES OF THE IRON ORE-DERIVED RED COLOUR PIGMENT

H.S.Woon[1]*,
L.S.Ewe[1],
K.P,Lim[2]
I. Ismail[3]

[1]College of Engineering, Universiti Tenaga Nasional (UNITEN), Malaysia, E-mail: hwoon@uniten.edu.my)
[2]Faculty of Science, Universiti Putra Malaysia (UPM), Malaysia, (E-mail: kplim@upm.edu.my)
[3]Institute of Advance Technology, Universiti Putra Malaysia (UPM), Malaysia,

Abstract: *This study proposes a novel technique to convert local iron ores into industrial grade red colour pigments. The methods employed in this work include high-energy milling, ball milling, rod milling and high-energy blending. It was observed in the TEM results that high-energy milling using ø 3 mm balls running at 550 rpm produced the finest particles with a value of 73.13 nm and a specific surface area of 178.62 m^2g^{-1} ,while ball milling and high-energy blending methods were similarly effective in producing nanoparticles with size of78.54 nm and 88.65 nm, respectively. The sample of high-energy milling at 550 rpm displayed noticeable alterations in colour values, but the lightness of high-energy blending samples was low in comparison to other methods. CIE L*a*b* colour values were analysed for all the samples and the results indicated that the value of a* for all the samples was greater than 18.0. This indicated that the samples are suitable for use as raw materials in red colour pigment production. Generally, the processing speeds utilized by the above mentioned methods resulted in significant changes in colour properties and its microstructure.*

Keywords: *Iron ore, Colour pigment; Ball milling; High energy ball milling; CIE L*a*b* colour values*

Introduction

Natural iron oxide colour pigments of high quality are confined to a limited amount of iron mines around the world. This is due to the difficulty of ensuring consistency within colour values as well as ensuring pigment performance properties of the harvested iron ores. Malaysian lands are well equipped with an abundance of iron ores [1-3]. However, research and development interests in harvesting, and converting Malaysia iron ores into colour pigments with quality have been frail, hence resulting in a loss of pace in the contention for valuable market shares in the pigment manufacturing industry, which is projected to expand over the next decade [4,8,11]]. As such, local producers of paints and other pigment-related products are dependent on foreign imports for pre-selected colour pigments, thus assuming a role of interim consumers in the supply chain and more susceptibility to global economic fluctuations and price changes. Furthermore, foreign imports with considerable quality come with expensive price tags [5-7]. The formation of new industries, job opportunities, lower costs, and increased profitability are potential advantages if raw materials such as iron ores were to be obtained from local sources.

Recently, the values of iron ores and steel products have been gradually dwindling due to reduction in construction and infrastructure development. This decline dampens the investment and development interests presented by local and international companies aiming to cater to the steel production industry in Malaysian ore-mining facilities [9,10]. The introduction of natural iron oxide pigments using local iron ores will serve as an alternative

product,or solution to the Malaysia mining and pigment industries. Moreover, the profit margins for local colour producers can be lucrative due to a high global demand, competitive pricing of colour pigments, and lowered iron ore prices [12].

The following issue can be tackled by presenting successful conversion of Malaysian iron ores into industrial grade colour pigments (particle size of 200 nm to 600 nm) by utilization of various size reduction methods such as high energy milling, high energy blending, ball milling and rod milling with different processing speeds aimed at studying its effects on the microstructures and colour values [13-15].

Experimental Procedure

The raw iron ores were obtained from iron mines in Malaysia. Elemental composition and phase stability of the raw iron ores were analysed as well as the type of iron oxide present in the ore samples prior to size reductions attributable to the utilized techniques. Presence of contaminants would significantly affect the quality of pigment and requires a tedious cleaning process. The X-ray diffraction (XRD), or the phase analysis was performed in order to detect the compound in the samples. This analysis was conducted by a CuKα (1.5418A) source (45 kV, 40 mA) from PANalytical Empyrean. The scans were executed with 2θ starting from 20^{o} to 80^{o}.

Upon completion of XRD, raw iron ores were hammered, and consecutively crushed into fine powder. The feed powder was then subjected to size reduction techniques with various speeds for different milling machines. High-energy ball milling, also known as planetary ball milling, was carried out in wet conditions, while the other techniques were performed in dry conditions. Subsequently, 5g of the feed powder was placed in a high-energy milling (Retsch, PM100) steel milling jar with distilled water. The charges used were steel balls with diameters of 3 and 11 mm. The machine was operated for 8 hours at 350 rpm and 550 rpm. In addition, a steel ball of diameter 5 mm was used for the conventional ball milling, while for the rod milling, steel rods with diameter of 7 mm and length of 134 mm were selected. Both ball milling and rod milling were operated at 64 rpm for 24 hours. Lastly, a high-energy blender (DM-6) was utilized at 25000 rpm for 5 minutes. The milling was conducted in a closed environment to secure the milling atmosphere.

Particle sizes of the milled powder were measured via a particle size analyser (Malvern Instruments Mastersizer 2000), based on the principle of evaluating the intensity of laser diffraction.. The powder was dispersed in water beforehand with the assumption of possessing a spherical particle shape. Specific surface areas of the samples was also evaluated with the use of the same machine.. TEM was further employed to confirm the particle size and particle shape. The evaluation of colour values were conducted by using a colourmeter (Konica Minolta CR 10) in order to provide measurements in terms of L*a*b*. The colourmeter was equipped with a gas-filled tungsten lamp as the light source and six silicon photocells as the detector.

Results and Discussions

The studies were carried out in accordance to three variables which included the following; average particle size (nm), specific surface area (m^2g^{-1}) and colour values. According to Figure 1, the the Ø 3mm ball had undergone a massive reduction from an initial value of 234.77 nm at 350 rpm to a final value of 73.13 nm at 550 rpm. In contrast, the Ø 11mm ball was observed to have reduced from 298.21 nm at 350 rpm to a final value of 231.30 nm at 550 rpm. What can be concluded is that the Ø 3mm ball was more effective in comparison to the Ø 11mm ball in high-energy milling of the iron oxide particles, especially with an increase in milling speed. A further conclusion is that incremental milling speeds allowed for small sized charge media to be used for optimal and effective size reduction processes. While the ball milling at 64 rpm

produced a sample with an average particle size of 78.54 nm, the DM-6 high-energy blender produced samples at an average of 88.65 nm. It can, therefore, be concluded that the calibration of suitable milling speed is a crucial factor affecting the particle size of iron oxide pigments.

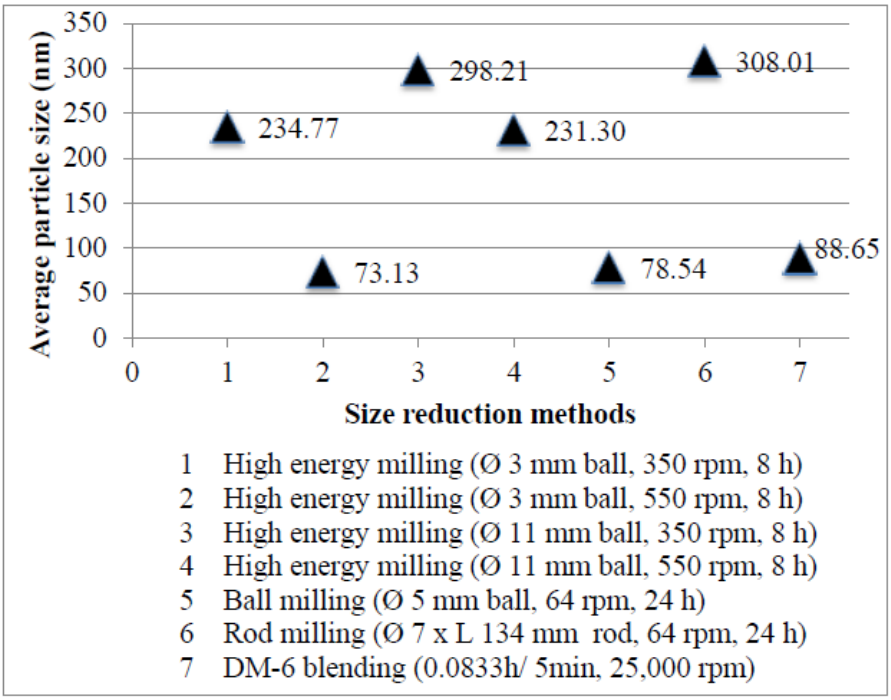

Figure 1: Average particle sizes with respect to size reduction methods

Regarding the specific surface areas, an increase in speed of high milling energy in both the Ø 3mm and Ø 11mm balls was observed to results in an increase in specific surface areas. Such a trend may also be applied to the high energy blending with 25000 rpm, which produced samples with a specific surface area of 103.05 $m^2g^{-1.}$ Regarding the ball and rod milling, the obtained specific surface area values were low due to the adjustment of the milling speed to 64 rpm. As shown in Figure 2 below, it may also be deduced that the changes in specific surface area was contributed to by speed variations in the size reduction methods.

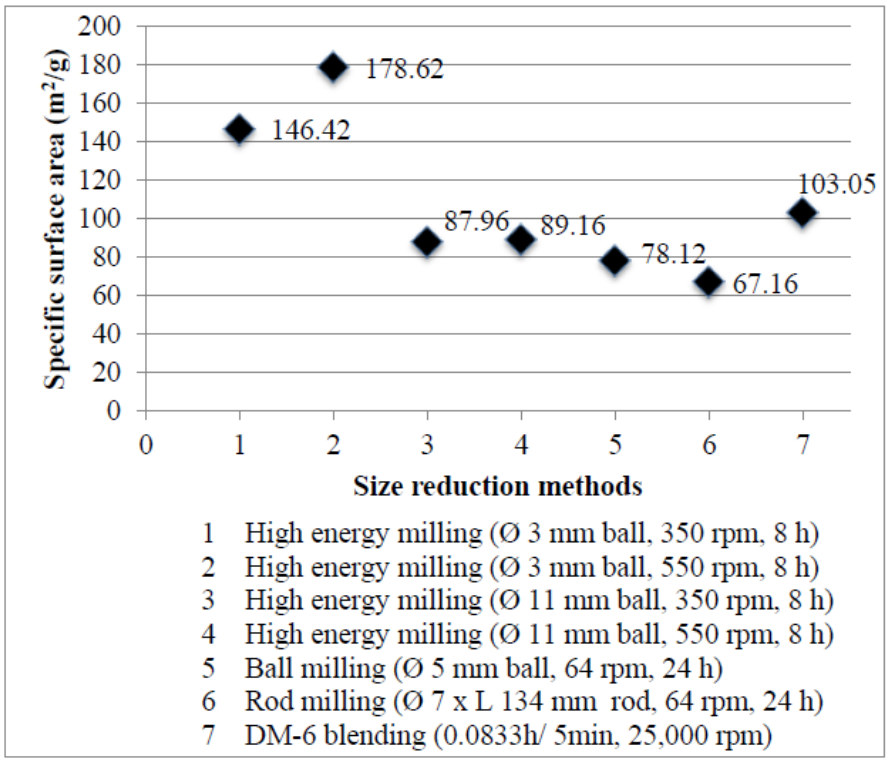

Figure 2: Specific surface area with respect to size reduction methods

It can be observed on Figure 4, in which Ø 11mm ball were utilized at 550 rpm, that the resulted particles were larger and formed larger agglomerates. This could be due to the low specific surface areas produced by high energy milling as an adsorptive gas layer could not form over each individual particle. In contrast, the particles in Figure 3 were smaller, exhibited less agglomeration, and produced more uniform-size particles. The milling speed in Figure 4 revealed that the particles were crushed in more effective manner. However, some of the particles were found as needle shaped.

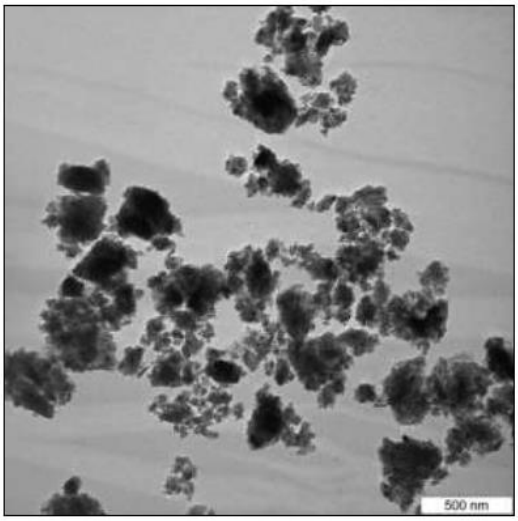

Figure 3: TEM image of high-energy milling (ø 3 mm ball, 550 rpm, 8 h)

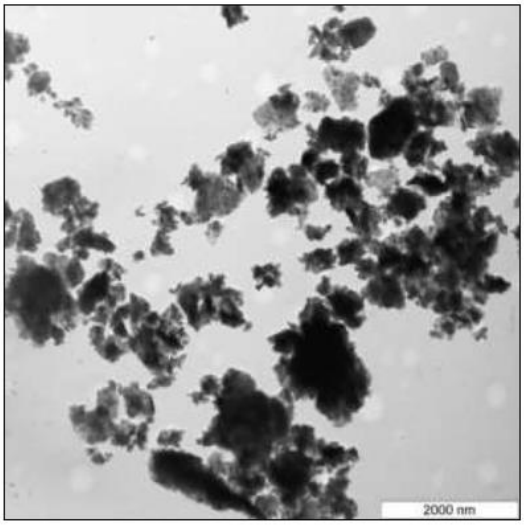

Figure 4: TEM image of high-energy milling (ø 11 mm ball, 550 rpm, 8 h)

Each size reduction method requires a unique milling speed in order to produce the desired particle size and shape. This could be observed as the high energy blending which produced rectangular particles, attributed to high random-manner collisions and particle-breakages in the blender. In contrast, the ball and rod milling process produced more circular and uniform particle shapes. This is attributable to slow milling speeds, which allowed the consistent milling pattern of these particle size distributions and shapes.

The lightness was highly noticeable at high-energy milling with 550 rpm, while the rod and ball millings were low in lightness as a result of the low speed. Furthermore, the high speed DM-6 blended samples exhibited lightness as well. This could be attributed to the differences in milling mediums between dry, versus wet, and the particle shapes differing between oval versus circular. A plausible explanation would be that the oval and circular iron oxide particles are more effective at light reflection and display of colour values. Figure 5 below displays an overview of the lightness recorded graph of the particles.

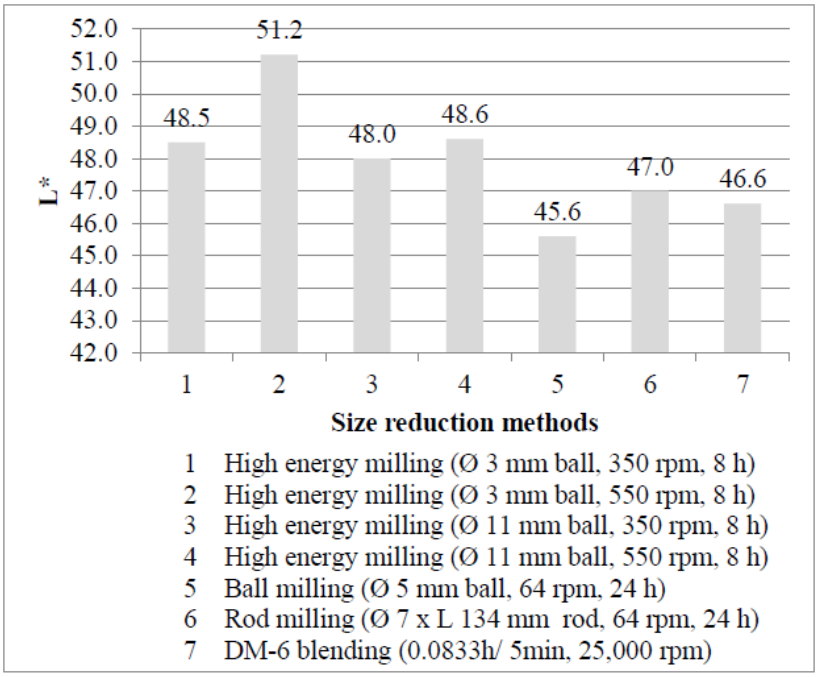

Figure 5: L* values with respect to size reduction methods

As for the redness or a* values of the particles, it was observed that the samples with high specific surface area tend to possess lower redness value. The high energy milling of the Ø 3mm ball with 350 rpm has the highest value of a* at 21.9 followed by Ø 11mm at 550 rpm which has a value of 20.6. The remaining values range from 18.7 to 19.9. Despite the higher specific surface area of DM-6, the sample had the lowest a* value at 18.7. This is likely attributable to the rectangular shape of the particles, which was unique to this sample and was possibly affected the redness display. The b* values of the high-speed conventional milling and DM-6 were similar, suggesting that both methods may produce samples with similar a* values. Selection of either methods depends on the particle shapes and sizes. Figure 6 and 7 below display the overview of both a* and b* values of the iron oxide samples.

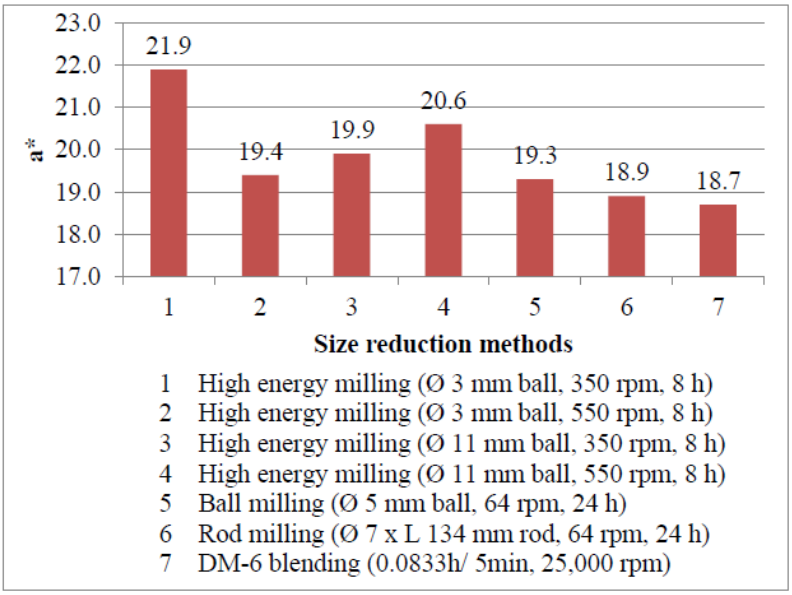

Figure 6: a* values with respect to size reduction methods

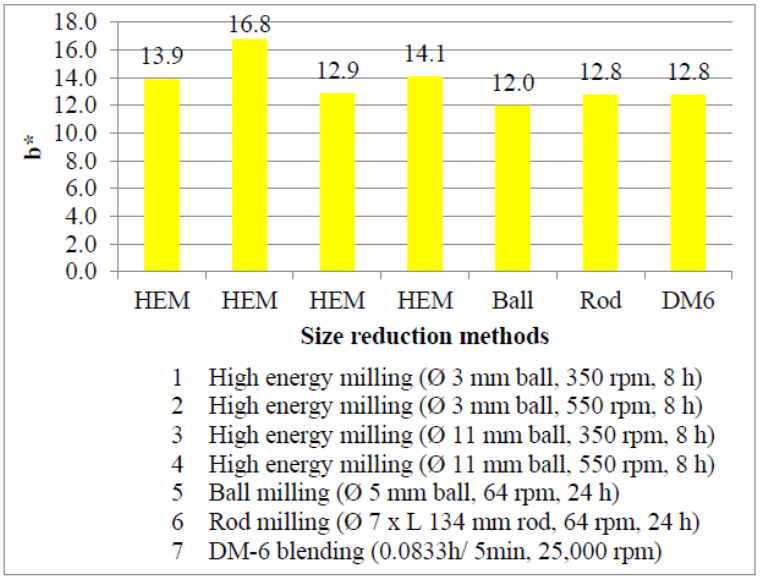

Figure 7: b* values with respect to size reduction methods

Conclusion

The obtained results of this study indicated that the value of processing speed in the various milling techniques is vital in the alteration of the particles sizes, as observed in the Ø 3mm and Ø 11mm balls at 550 rpm, which had noticeable average size reductions. Furthermore, it was concluded that reduction in particle sizes results in higher value of specific surface area. It was concluded that high-energy milling using ø 3 mm balls running at 550 rpm and high-energy blending at 25000 rpm could successfully produce particles with sizes less than 100 nm. Moreover, results indicated that the red colour properties (a* values) were best produced by the high-energy milling.

References (APA Sixth Edition, Single Spacing)

1. Wong, Y.W., Woon, H.S., & Tan, C.Y. (2014). Purification and conversion of Malaysian iron ores into industrial grade iron oxide colour pigment, *Materials Research Innovations*, 18, 5-13.
2. Tian, G., Wang, W., Mu, B., Wang, Q. and Wang, A. (2017). Cost-efficient, vivid and stable red hybrid pigments derived from naturally available sepiolite and halloysite. *Ceramics International.* 43, 1862-1869.
3. Koltsov, A., Cornu, M.J., Nicolas, S., Colom, L., and Dossot, M. (2014). Behaviour of tetra mine inhibitors during pickling of hot rolled steels. Applied Surface Science, 293, 24-36.
4. Yue, Y.Y., et al. (2016). Descaling Behaviour of 430 Hot-rolled stainless steel in HCL based solution. Journal of Iron and Steel Research. 23, 190-196.
5. Zhang, Z., Zhang, Q., Xu, L., and Xia, Y. (2007). Preparation of nanometer γ-Fe_2O_3 by an electrochemical method in non-aqueous medium and reaction dynamics, *Synthesis and Reactivity in Inorganic, Metal-Organic and Nano-Metal Chemistry*, **37**, 53-53.
6. Bang, J.H., and Suslick, K.S. (2007). Sonochemical synthesis of nanosized hollow hematite, *J. Am. Chem. Soc.*, **129**¸ 2242-2243.
7. Prim, S.R,. at el (2011). Synthesis and characterization of hematite pigment obtained from a steel waste industry. *Journal of Hazardous Materials*, 192, 1307-1313.
8. Riveros, P.A., and Dutrizac, J.E. (1997). The precipitation of hematite from ferric chloride media, *Hydrometallurgy*, **46**, 85-104.
9. Love, C.H. (1973). *Pigment handbook*. New York, John Wiley & Sons Inc.
10. Podolsky, G., and Keller, D.P. (1994). *Industrial minerals and rocks*. Littleton, CO, Society for Mining, Metallurgy and Exploration.
11. Stoye, D., and Freitag, W. (1998). *Paints, coatings and solvents*, Weinheim, Wiley-VCH.
12. Sugimoto, T., and Sakata, K. (1992) Preparation of monodisperse pseudocubic α-Fe_2O_3 particles from condensed ferric hydroxide gel. *J. Colloid Interf. Sci.*, **152**, 587-590.
13. Wang, W. et al. (2017). Novel environmental friendly inorganic red pigments based on attapulgite, *Powder Technology*, 315, 60-70.
14. Marinoni, N., and Broekmans, M.A. (2017). Microstructure of selected aggregate quartz by XRD and a critical review of the crystallinity index, *Cement and Concrete Research*, 54, 215-225.
15. Allegratte, I., Pinto, D., and Eramo, G. (2016). Effect of grain size on the creativity of limestone temper in a kaolinitic clay. *Applied Clay Science*, 126. 223-234.

International Conference on Modern Applied Sciences, Engineering and Technology Application 2019 (ICMASET 2019)
eISBN: 978-967-2245-16-2
25th - 26th September 2019,
Bayview Beach Resort, Penang, Malaysia

ASSESSMENT ON THE NEGATIVE IMPACT OF THE SHIELDING EFFECTIVENESS OF THE METAL ENCLOSURE OF A WIRELESS ACCESS POINT AND IMPROVEMENT

Mohd Zairil Zainal[1]
Xavier Ngu Toh Ik[2]
Meizareena Mizad[3]

[1]Information Technology Centre, Universiti Tun Hussein Onn Malaysia (UTHM), Malaysia, (E-mail: zairil@uthm.edu.my)
[2]Faculty of Electric and Electronic, Universiti Tun Hussein Onn Malaysia (UTHM), Malaysia, (Email: xavier@uthm.edu.my)
[3]Centre for Language Studies, Universiti Tun Hussein Onn Malaysia (UTHM), (E-mail: meizareena@uthm.edu.my)

Abstract: *This study was done to identify the negative impact of the shielding effectiveness of the metal enclosure of a Wireless Access Point (WAP). In these study radio waves propagation will be considered using the Wireless LAN (WLAN) 802.11n at the frequency of 2.4GHz. The study involves the effect on the type materials used for the enclosure to secure the WAP. A comparison was made between the two materials which are metal and polylactic acid (PLA) as the enclosure of the Wireless Access Point. The methodology used in this research are; by using experimental study which was performed at the Electromagnetic Center (EMC). Based on the results, it was concluded that potential interference exists by using the metallic materials which reduces the performance of the WAP. Thus, the aim of this study is to design and produce a new enclosure with less interference.*

Keywords: *Shielding, Metal Enclosure, PLA Enclosure*

Introduction

Nowadays, the use of wireless network technology is rapidly gainning popularity in order for people to get connected to the network. A client revolution such as tablet, smartphone and laptop lead to an access network revolution from wired to wireless network [4]. Bring Your Own Device (BYOD) gives a greater impact for the wireless network usage. BYOD assists many staff and students in becoming well-informed on the changing technology by using their own personal devices like laptops and/or smartphones from home or colleges and using them both for study/work and personal purposes. Thus, with BYOD people can be easily get connected with the network to stay up-to-date.

The WLAN technology 802.11(a/b/g/n) are already being used in Universiti Tun Hussein Onn Malaysia (UTHM). The WLAN technology namely the Wireless - Fidelity (Wi-Fi) for the staff and students to access networks using mobile devices. These facilities are available to improve the quality of teaching and learning at the university. Apart from that, the facilities are provided to promote the e-learning culture among lecturers and students of UTHM.

One of the requirements to provide the WLAN services is by using the Wireless Access Point (WAP) [7]. There are 526 units of WAP 802.11(a/b/g/n) with various models have been installed at the campus and residential colleges in UTHM. The models of the WLAN are Aruba model 175, 115, 135, 125, 105, 93, 85, 80, 61 and 60. All the WAP installed is included with metal protection systems in order to improve the safety and to avoid from being stolen and vandalized.

Apart from that, complaints were often made by the users of UTHM regarding to the low wireless signal. Based on the data collected from the year 2017 to 2019 at the Information Technology Centre (ITC), there was a huge number of complaints that is 799 in the consecutive years. The highest number of complaint made by the users is 298 in 2018 as shown in figure 1. The interference of wireless signal was found to be the main cause of Wi-Fi complaints.

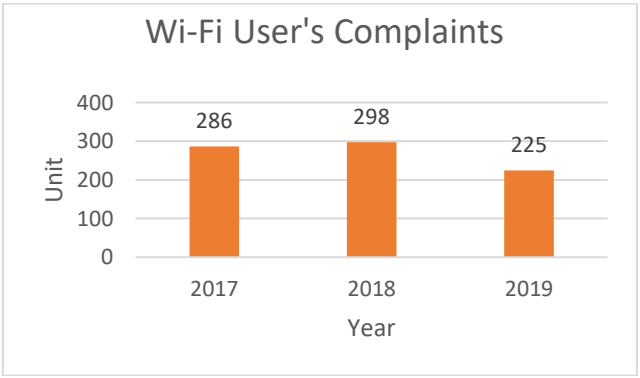

Figure 1: Wi-Fi Users' Complaints
Source: Ticketing System UTHM

These complaints were mostly referring to WAP operating at 2.4GHz radio frequency. The radio frequency wave is sensitive to building material. It can be attenuated, diffracted, and reflected when it passes through obstacles such as metal surfaces, wood wall, brick wall, roofing and glass [3] and [4]. Reflection, diffraction and scattering will occur on the radio waves propagating through the building material. In this study, the metal enclosure, as shown in figure 2, used to secure the WAP is the source of the problem.

There were two (2) major problems occurred on the WAP with radio frequency 2.4 GHz:

i. The metal enclosure used for the WAP resulted in interference on the wireless signal.

Figure 2: Metal Enclosure for the Aruba WAP 105 model
Source: Ticketing System UTHM

ii. The performance of the WAP decreased because the metallic materials used as the enclosure create interference and obstacle to the wireless signal.

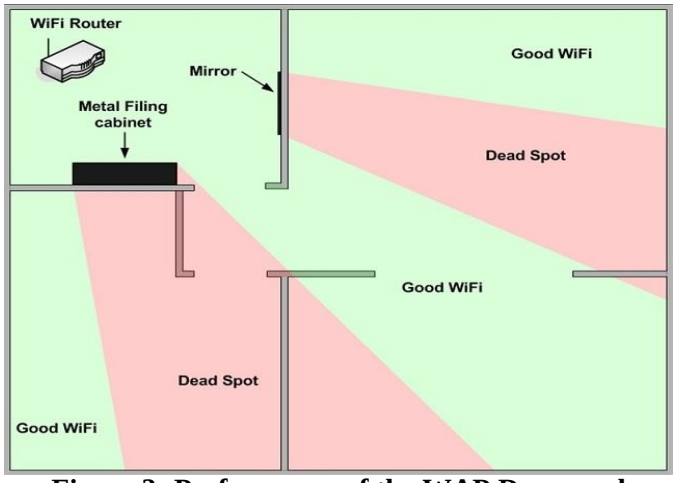

Figure 3: Performance of the WAP Decreased
Source: Ticketing System UTHM

Even though most applications of the new technologies such as commercial of the shelf (COTS) and low-cost wireless communication technology are for the architectures typical of a business enterprise, the transportation of nuclear materials inside an important metal transport or vehicle is needed to be monitored wirelessly [1]. Practically, the metal that is used as the materials in the environment has led to complication in the wireless communication. The study was carried out to focus on 2.4GHz transmission spectrum and wireless data communication within a metal transportation vehicle. Based on the other observation by the researcher, the omnidirectional antenna is the most homogeneous and consistent elevated results across all configurations of containers while the flat patch-panel antenna appears to be more sensitive to directions [1]. Therefore, to overcome the problem of wireless communication, it is not suitable to use WAP 2.4 GHz radio frequency with flat patch-panel antenna together with the metal enclosure.

There was another research done pertaining to the use of metal materials as the enclosure of the WAP. In the study, the researcher hypothesized that the structure of the metal such as bus lines or power lines which is near to the antenna would cause a significant disruption and affects the antenna features [2]. Therefore, the researcher found that to overcome this, the metal structure that is attached directly on the antenna should be avoided because it will change the network. Based on evaluation of the structures, a set of design guidelines for reducing the impact of the structures has been developed. Thus, in this study to cater the interference signal in the wireless communication, a new prototype design for enclosure has to be produced with less of metallic materials.

Wireless signal propagation mechanism is refers to how the wireless signal is transmitted. Propagation mechanism refers to how the signal is being propagated [4]. There are three (3) types of propagation mechanism that affect the signal transmission which are reflection, scattering, and diffraction. Reflection occurs when the wave encounters an object of large dimension as compared to its wavelength such as large walls, metal cabinets, ceilings and furniture. Scattering occurs when the transmitted have encountered a large quantity of small dimension objects such as metal cabinets, lampposts, bushes and trees. Diffraction occurs when the surface of the obstruction has sharp edges producing secondary waves that in effect bend around the obstruction [4]. Thus, one of the materials in metal such as metal cabinet will cause reflection and absorption of signal to occur. Figure 4 shows the three (3) types of propagation mechanism.

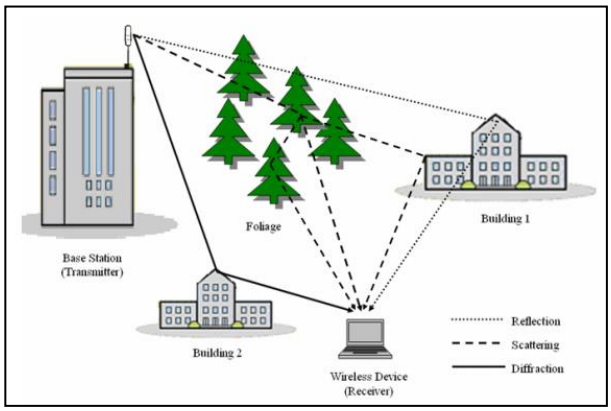

Figure 4: Three types of propagation mechanism
Source: Ali, A. H., Razak, M. R. A., Hidayab, M., Azman, S. A., Jasmin, M. Z. M., & Zainol, M. A. (2010, October). Investigation of indoor WIFI radio signal propagation.

The loss of wireless signal propagation is depending on the materials used for buildings. It is very crucial to understand the propagation of radio wave signals to come up with an appropriate design, deployment, and management for any wireless network. There was a loss of wireless signal towards the barriers of building materials.

Table 1: Common objects and corresponding attenuation in dB

Obstacle	2.4 GHz (dB)
Interior drywall	3-4
Cubicle wall	2-5
Wood door (Hollow - Solid)	3-4
Brick / Concrete wall	6 – 18
Glass / Window (not tinted)	2-3
Double-pane coated glass	13
Bullet-proof glass	10
Steel / Fire exit door	13-19

Source: RF Basics - Part 1 - Aruba Networks. (2017, June 9)

Table 1 displays the loss (or attenuation in dB) presented by several objects. Most of the attenuation numbers are given as a range; the actual value of the attenuation depends on the exact frequency on transmission, the thickness and also the specific type of material used. Thus, the measurement conditions may be different as the numbers measured at different locations do not always agree. The attenuation numbers for concrete walls are seen as the most controversial because of the different types of concrete materials used and the thickness and coating are differed depending on whether it is used in floors or interior or exterior walls [8]. Generally, brick walls have attenuation at the lower end of the range as shown in the table below.

Thus, the attenuation of signals can occur depending on the obstacles that exist at the surrounding area. At some point, the system receives fair signals; it is due to the fact that different machines produce noise which effect the Wi-Fi signal [3].

Methodology

The purpose of this research is to identify the implication and differences on the metal enclosure used on the 2.4GHz radio frequency transmission antenna. The experiment was done in the Electromagnetic Centre.

Initial experiments were conducted to observe the performance of the 2.4 GHz antenna in the Aruba WAP 105 model when operating together with the metal enclosure. The flow of the work can be described in three steps.

i. Initial experiments were conducted in the EMC to observe the radiation pattern of the wireless signal propagation produced by using 2.4GHz antenna without the metal enclosure.
ii. The metal enclosure will then be installed together with the WAP and the new radiation pattern was observed to examine the impact of the enclosure on the wireless signal propagation.
iii. A prototype enclosure made of plastic material (Polylactic Acid - PLA) will be designed. The enclosure is designed using CAD software to obtain three-dimensional (3D) profile in which shall beprinted using a three-dimensional printers (3D). This Polylactic Acid (PLA) enclosure will be tested with 2.4GHz antenna in the EMC to observe the impact on the wireless signal propagation.

The data collected from these three (3) methods will be analyzed to identify the difference and implication for 2.4 GHz on the particular material that was used as the enclosure.

Analyses

From the experiments conducted, the radiation pattern without the enclosure is shown in Figure 5. It displays that the radiation pattern of the wireless signal propagation produced by the 2.4GHz antenna without the metal enclosure is a reasonably nice circle, suggesting that the omnidirectional antenna is good and performing the job as it intended to.

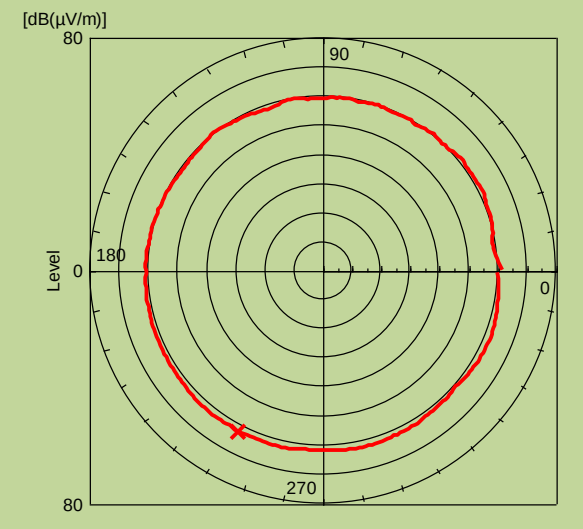

Figure 5: Radiation pattern for a 2.4Ghz Antenna without Metal Enclosure
Source: Electromagnetic Centre Laboratory UTHM

Subsequent test was done to observe the radiation pattern of the wireless signal propagation produced by the 2.4GHz antenna with the metal enclosure installed. the radiation pattern is now being distorted. It can be observed that, the distortion occurs at the angle between 90 degree and 280 degree. Figure 6 below shows the radiation pattern after the experiment was

performed. The distortion occurring at these angle can be explained by the heavily shielded area of the enclosure which is at the sides of the enclosure. On the other hand, a good pass through is observed towards the front of the enclosure and this is mainly due to the large opening which permits waves to pass through unobstructedly.

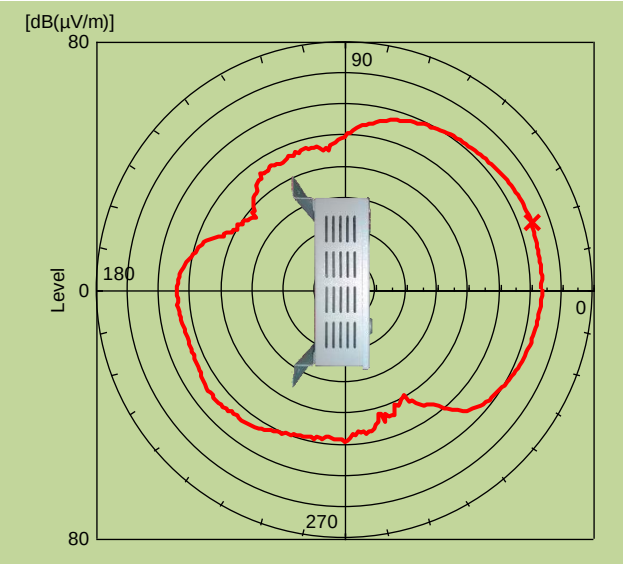

Figure 6: Radiation pattern for a 2.4GHz Antenna with Metal Enclosure
Source: Electromagnetic Centre Laboratory UTHM

A final test was conducted by using the 2.4GHz antenna with the PLA enclosure. The result shows that the radiation pattern has indeed returned into the circle shape as per the first experiment, even though not exactly similar. This probably suggests that minor interference still exist, but not as strong as compared to that of metal enclosure. .. Figure 7 shows the radiation pattern for the WAP with PLA enclosure.

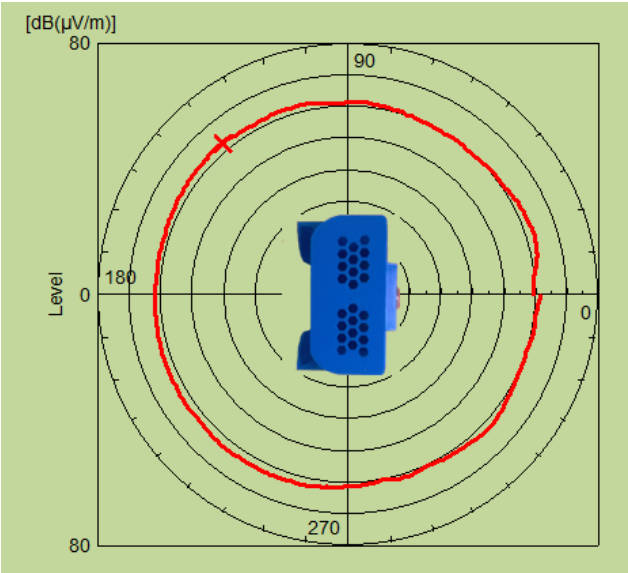

Figure 7: Radiation pattern for a 2.4GHz Antenna with PLA Enclosure
Source: Electromagnetic Centre Laboratory UTHM

Conclusion

This study concludes that the PLA has a better suitability being the material to be used as a shielding enclosure for 2.4GHz antenna. On the other hand, the suitability of the material to withstand vandalism still require further work. More subsequent work will be performed to fully understand the PLA material such as the designs and its strength so that a compromise can be achieved in both directions that are to achieve a good transparency to radio waves and at the same time strong enough to be use as a protection enclosure for Wireless Access Point.

References

[1] Cooley, H.T., "IEEE 802.11, OpenAir and HomeRF for 2.4 Ghz spread-spectrum wireless data communication within a metal transportation vehicle," Security Technology, 2004. 38th Annual 2004 International Carnahan Conference on, vol., no., pp.204, 211, 11-14 Oct. 2004.A.,

[2] Xiaoling Guo; Ran Li; O, K.K., "Design guidelines for reducing the impact of metal interference structures on the performance on-chip antennas," Antennas and Propagation Society International Symposium, 2003. IEEE , vol.1, no., pp.606,609 vol.1, 22-27 June 2003.

[3] Sohail, Ahsan, Zeeshan Ahmad, and Iftikhar Ali. "Analysis and Measurement Of Wi-Fi Signals In Indoor Environment 1." vol. 6, Issue 2, pp.678-687, May 2013.

[4] Ali, Abdul Halim, MR Abd Razak, Muzaiyanah Hidayab, Syuwari Ashraf Azman, Mohd Zaim Mohd Jasmin, and Mohd Azmir Zainol. "Investigation of indoor WIFI radio signal propagation." In Industrial Electronics & Applications (ISIEA), 2010 IEEE Symposium on, pp. 117-119. IEEE, 2010.

[5] Apple (2007). Wi-Fi and Bluetooth: Potential sources of wireless interference." Learn about potential sources of Wi-Fi and Bluetooth (wireless) interference. from http://support.apple.com/kb/ht1365.

[6] Ruey Bing Hwang; Ta Chun Pu, "A Planar Shaped-Beam Antenna for Indoor Wireless LAN Access Points," *Antennas and Propagation, IEEE Transactions on* , vol.55, no.6, pp.1871,1879, June 2007

[7] Delannoy, P.; Marot, M.; Becker, M., "WiMax quality-of-service estimations and measurement," Wireless Communication, Vehicular Technology, Information Theory and Aerospace & Electronic Systems Technology, 2009. Wireless VITAE 2009. 1st International Conference on , vol., no., pp.503,509, 17-20 May 2009

[8] RF Basics - Part 1 - Aruba Networks. (2017, June 9). Retrieved from https://community.arubanetworks.com/t5/Wireless-Water-Cooler/RF-Attenuation-Values-of-typical-Building-Materials/td-p/298939

International Conference on Modern Applied Sciences, Engineering and Technology Application 2019 (ICMASET 2019)
eISBN: 978-967-2245-16-2
25th - 26th September 2019,
Bayview Beach Resort, Penang, Malaysia

ANALYSIS OF WIND WITH BATTERY CONNECTED TO MICROGRID SYSTEM

Alias Khamis[1]
Mohd Ruddin Ab. Ghani[2]
Chin Kim Gan[3]
Mohd Shahrieel Mohd Aras[4]
Azri Bin Jaafar[5]

Faculty of Electrical Engineering Universiti Teknikal Malaysia Melaka
[1]alias@utem.edu.my, [2]dpdruddin@utem.edu.my,
[3]ckgan@utem.edu.my,[4]Shahrieel@utem.edu.my,[5]azri@utem.edu.my

---

Abstract: *Nowadays, distributed generation technology had gained more popularity by many countries. Recently, there are many problem with power system. One of the problem is high electricity price. The price in power generation rely largely on the type and market price of the fuel used, government subsidies, government and industry regulation, and even local climate patterns. In order to supply a better power system, this thesis introduces a model of wind turbine and a battery storage connected to microgrid system. The microgrid is the small scale which widely used in power generation system. Microgrid can operate with renewable and non-renewable energy. Through this project, microgrid will be modelling by using wind turbine and battery storage system using MATLAB simulink software.*
Keywords: *Battery Storage, Grid connected, Microgrid and Wind Tubine*

Introduction

This project shows the analysis of distribution generation (DG) units refer to the small generators that used as stand-alone systems at an isolated area (rural areas) or utility-connected. It is having the ability to lift the poor nations to new levels of prosperity. The renewable energy used in this project is wind turbine. Basically the wind turbine generates from the sources of airflow through mechanical power generator to electricity. This wind turbine suitable at offshore and large area. Offshore had wind more frequent and stronger which can be found at this location and have less impact on the landscape aesthetic than project land but the cost of construction and maintenance costs are high.

There are several issues make this project build up. One of the issue are by using the fossil, coal, oil and natural gas generation to generate electricity. Based on the fossil fuel generation, the fossil will have burned and from that the nitrogen oxide come out to surrounding. It is make the acid rain and effect the greenhouse gas emission. It is also make air pollutant. Besides that, a regular problem in industry when using traditional grid that only ways to flow electricity and communication. The other way by using microgrid that have reliability and secure network and loads with provide efficiency and friendly environment.

Wind Turbine

Wind energy is renewable energy. It is a clean energy source without requiring chemicals such as oil to generate energy which enable pollution. Wind energy is a source that needs wind to generate electricity. Wind turbines operate on a simple principle. The energy in the wind turns two or three propeller-like blades around
a rotor. The rotor is connected to the main shaft, which spins a generator to create electricity. The formula for output power of wind turbine is

$P = ½ * \rho * C * A * v^3$

Where
ρ is air density that normally use is 1.23
C is maximum power coefficient; theoretical maximum is 0.59 A is area of rotor
v is wind speed or velocity
Wind turbine configuration can be identifying many ways based on different factors such as:

- Rotor axis orientation: horizontal and vertical
- Rotor position: upwind or downwind of tower
- Rotational speed: constant or variable
- Rotor power control: pitch, stall and active stall

Figure 1: Example of Horizontal Axis Turbine Wind Turbine3.

Figure 2: Example Vertical Axis Wind

The Horizontal Axis Wind Turbine
A horizontal-axis wind turbine (HAWT) has the main rotor shaft and electrical generator at the top of a tower and point directly into the direction of wind. Small turbines are pointed by a simple wind vane, while large turbines use a wind sensor coupled with a servo motor. Most system has a gearbox, which turns the blades slow rotation into a quicker rotation that is more suitable for generate electricity. Turbine blades are made stiff to prevent the blades from being pushed into the tower by high winds.

Vertical Axis Wind Turbine
Vertical-axis wind turbines (VAWT) have main rotor shaft running vertically. Main advantages of this arrangement are the generator and/or gearbox can be placed at the bottom which near the ground. So the tower does not need to support it and the turbine does not need to be pointed into the wind. Vertical wind turbines have a higher airfoil pitch angle to give improved aerodynamics while decreasing drag at low and high pressures.

Microgrid
Microgrids have ability to enhance there liability of the electric power grid from the point of view of their local loads means that the uninterruptable and high quality power is delivered to the loads, particularly critical loads. Microgrid can provide reactive power to support local voltage levels (415VL-L) not only for their own local loads but also for nearby loads. Microgrids is operate in parallel with the utility grid to feed a certain load. This prevents the grid being overloaded during peak load periods, which may consequently result in blackouts. By using microgrid,it can reduce the transmission losses (economic benefit) means the power that delivered to areas where microgrids are installed are lower and losses on the lines are lower too.

Battery Storage

A battery stores electrical energy in a dual direction chemical reaction. The renewable energy source produces the energy and the battery stores it for times of low or no renewable energy production. Most renewable energy systems have batteries which store between ten and hundreds of times more energy than a car battery. It need backup power in case batteries become discharged due to lack of renewable energy system or an over consumption of energy.

There are many brands and types of batteries available for renewable energy systems. With proper care, renewable energy system batteries have a lifetime of five to ten years, but there are more expensive batteries. In batteries consists of dangerous chemicals, which is hydrogen and oxygen gas while being charged, so they should be vented to the outdoors. It tops and connections must be periodically cleaned to avoid energy losses. Batteries should also be regularly topped up with distilled water.

The lead acid battery used as energy storage because the lead acid battery is common energy storage device for renewable energy sources with high power density. Several inputs are considered for the modelling of this battery such as battery current, capacity, state of charge and temperature. All these parameters are varied with the operating conditions and affected the capacity of battery to charge or discharge. The battery terminal voltage is considered as an output of the model.

Design of Wind Turbine and Battery Storage Connected with Microgrid in Grid-Connected and Grid-Disconnected

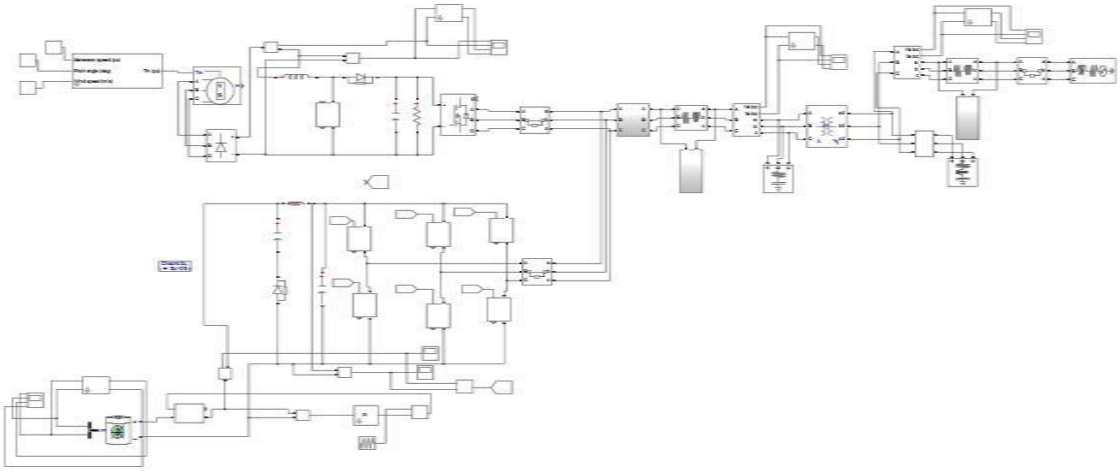

Figure 3: Design of Wind Turbine and Battery Storage connected with Microgrid in Grid-connected and Grid-disconnected

Based on figure 3, the wind turbine and battery storage connected with grid. There are rectifier and converter that used after wind turbine and battery storage. Its function to compatible in voltage and frequency with electronic power system to which it will be connected and contain necessary output filter. The filter used is LC filters which to smooth the graph and filter noise to obtain synchronous voltage and frequency. Before transmit to Microgrid, the supply need transformer to step-up the voltage to synchronize with Microgrid due to frequency and voltage. The grid voltage is 415V and the frequency is 60Hz. The supply will go through the load demand.

Microgrid in Grid-Connected and Grid-Disconnected Mode

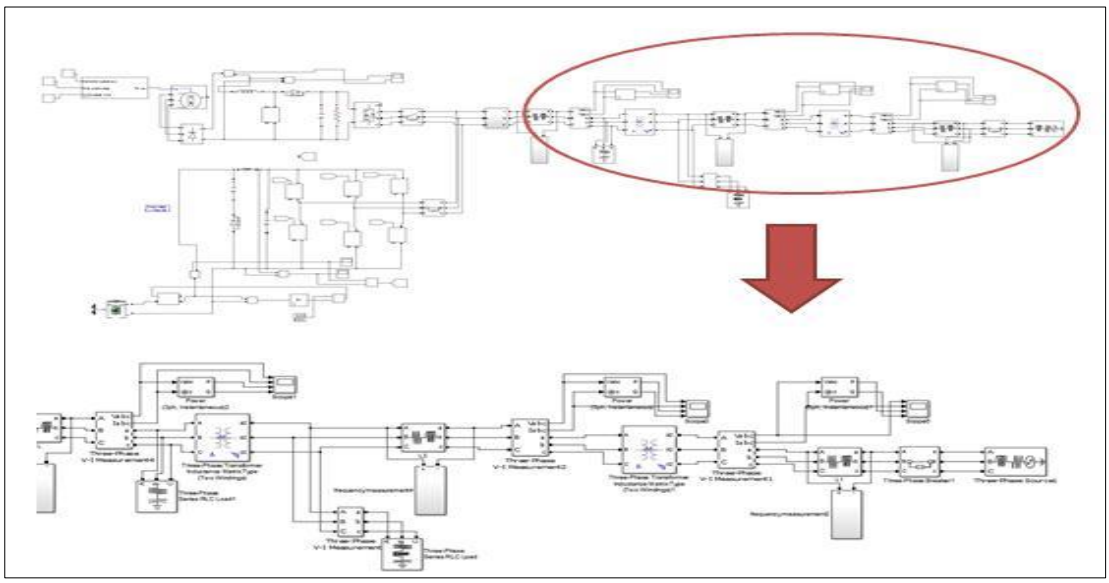

Figure 4: Design of 11kV Microgrid

Figure 4 shows the design of 11kV microgrid. The grid is added after the 415V side to become 11kV. It related with supply from wind turbine and battery storage and then the transformer is step up the voltage to 415V. After that the 415V where step up again until to 11kV. The reading is taken at 415V side and 11kV side. There have 2 condition of grid which is grid-connected and grid-disconnected. The breaker is placed at 11kV grid to connect or disconnected the grid.

Result and Discussion

Wind And Battery Storage Connected With GridConnected And Grid-Disconnected

Based on figure 3, show the distributed generation of wind turbine and battery storage connected with Microgrid. When this Microgrid system in grid-connected, the breaker will CLOSE means the grid can gives supply for the system. Meanwhile, if the Microgrid system in grid-disconnected, the breaker will OPEN means the grid cannot give supply for this system. The design were stimulate based on different cases which are

1. Wind turbine supply to grid connected
2. Battery supply to grid connected
3. Wind turbine and Battery supply to grid connected
4. Wind turbine supply to grid disconnected
5. Battery supply to grid disconnected
6. Wind turbine and Battery supply to grid disconnected

Case 1

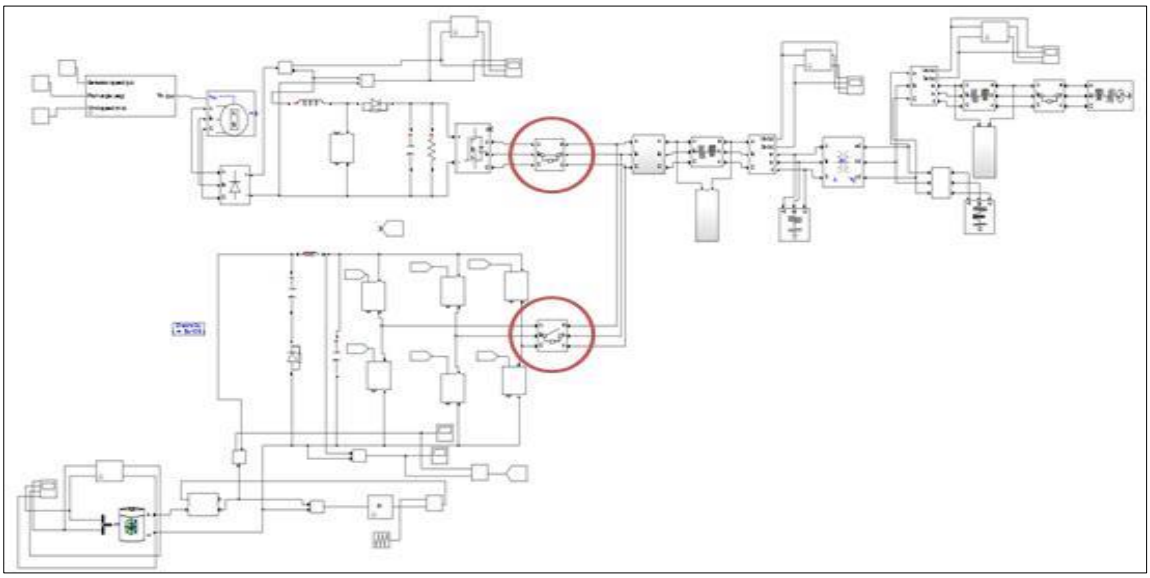

Figure 5: Wind Turbine Supply in Grid-connected

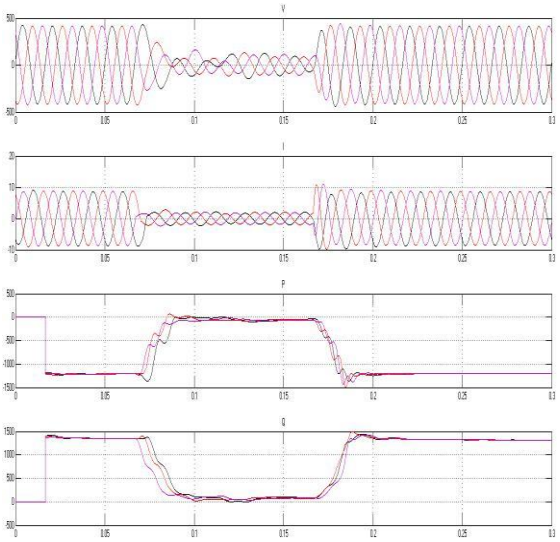

Figure 6: Result of Primary voltage, current, active power and reactive power

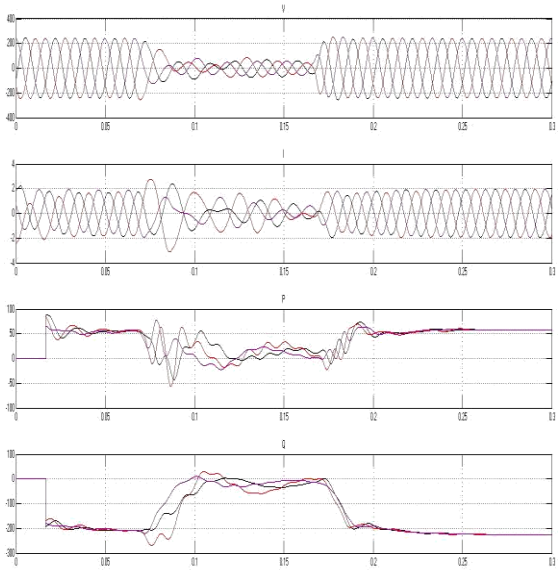

Figure 7: Result of Secondary voltage, current, active power and reactive power

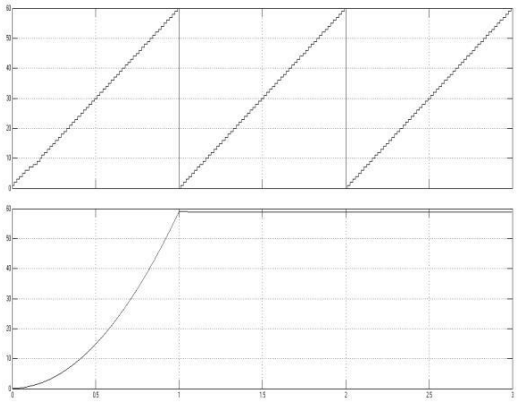

Figure 8 Result of Frequency

Case 2

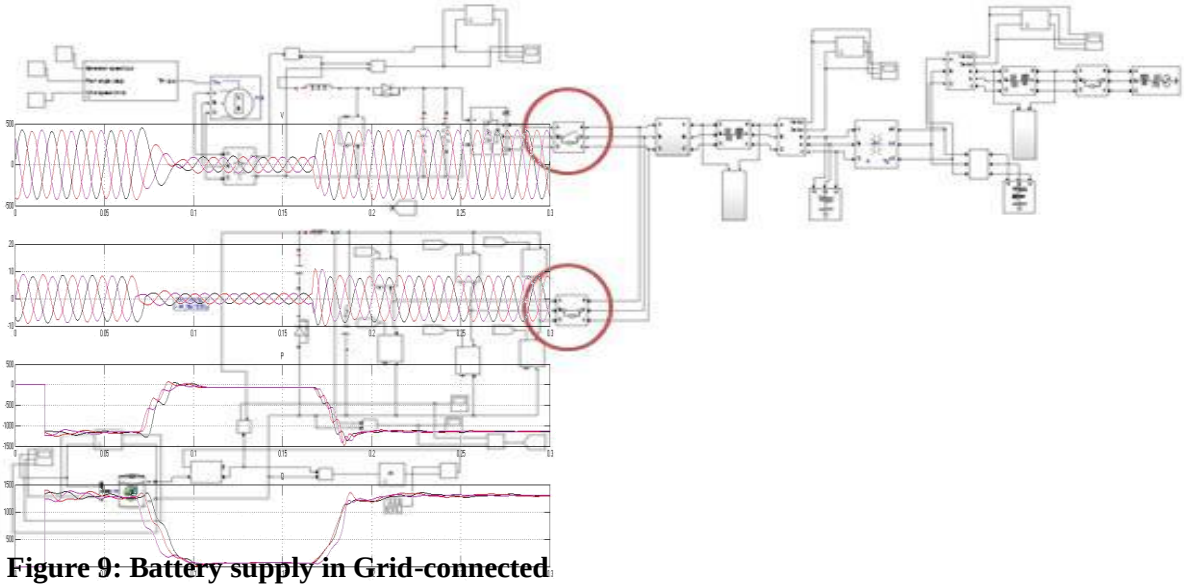

Figure 9: Battery supply in Grid-connected

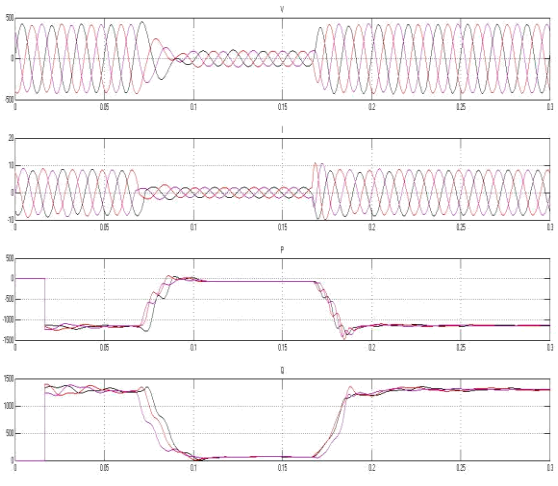

Figure 10: Result of Primary voltage, active power and reactive power

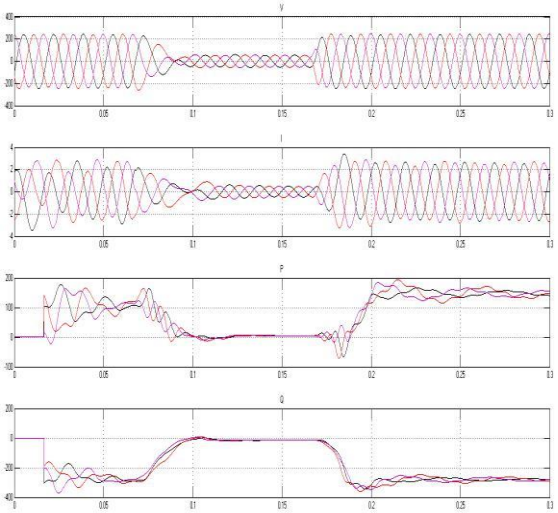

Figure 11: Result of Secondary voltage, current, current, active power and reactive power

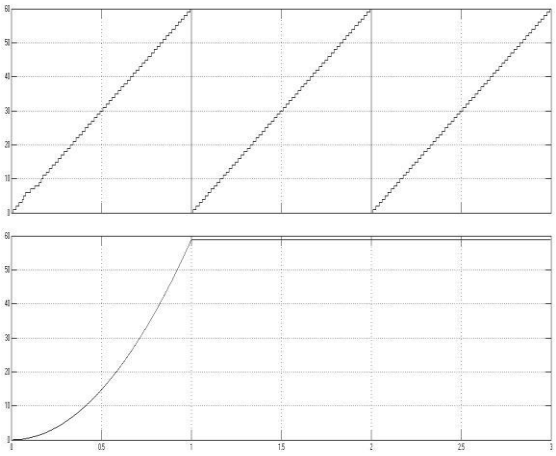

Figure 12 Result of Frequency

Case 3

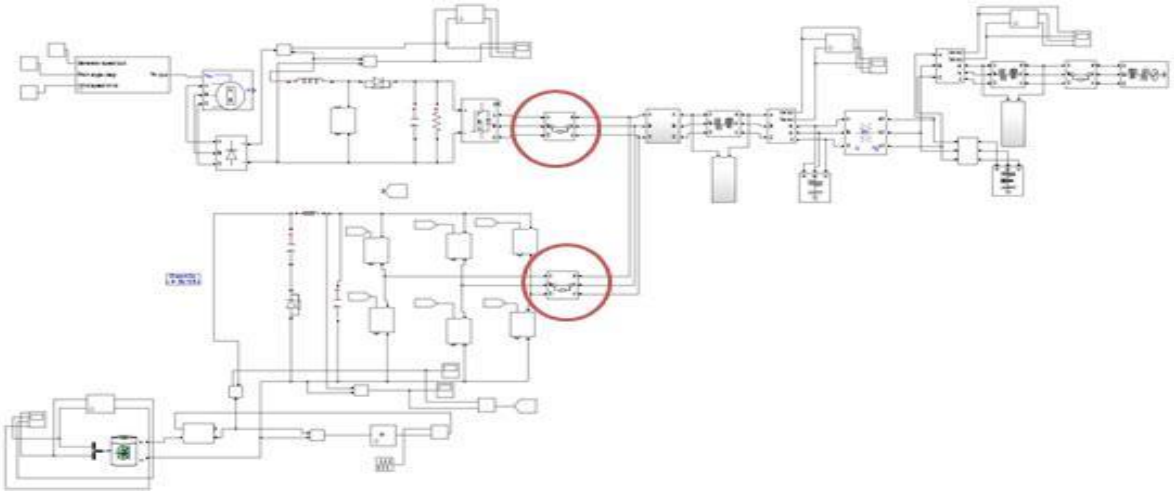

Figure 13: Wind turbine and Battery supply in Grid-connected

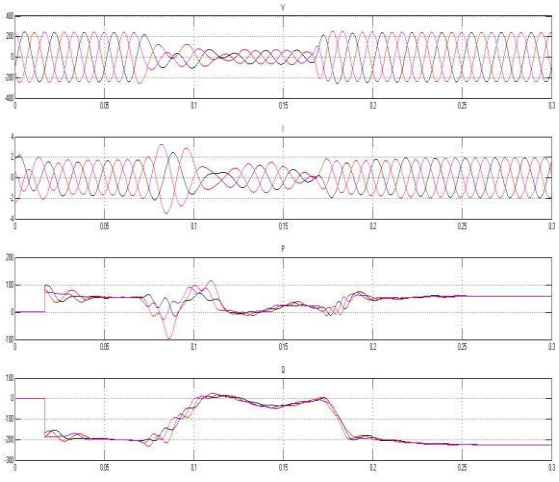

Figure 14: Result of Primary voltage, current, active power and reactive power.

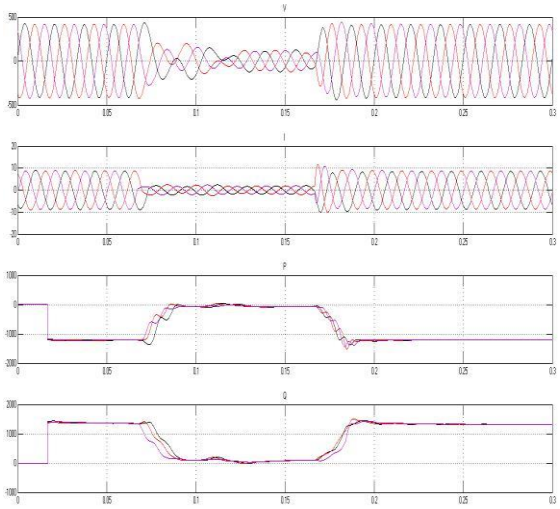

Figure 15: Result of Secondary voltage, current, active power and reactive power

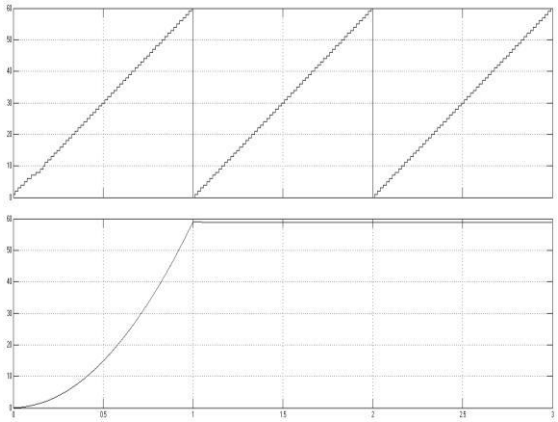

Figure 16 Result of Frequency

Case 4

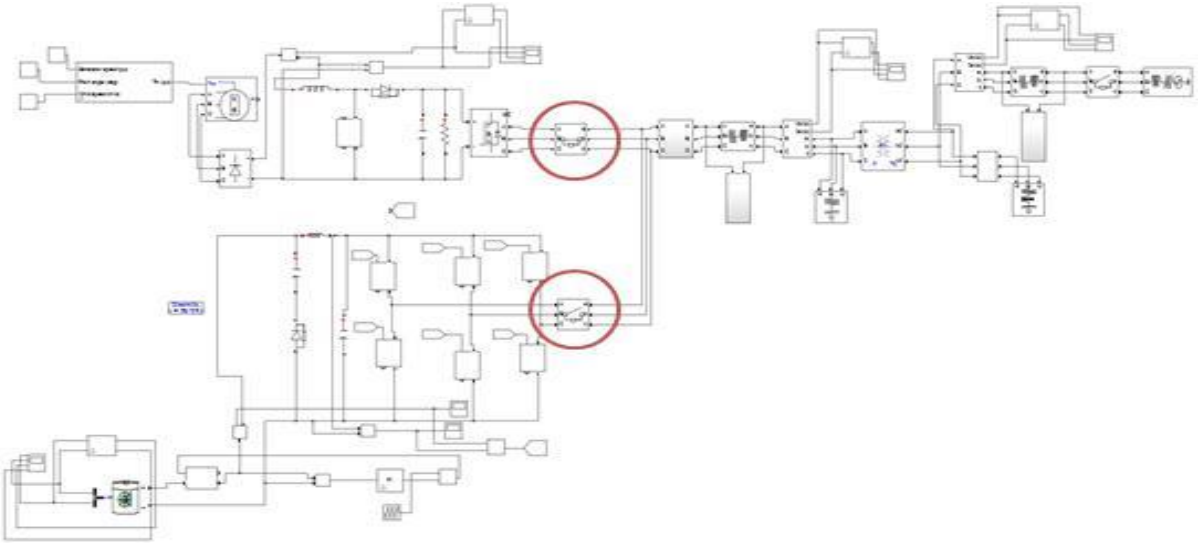

Figure 17: Wind turbine supply in Grid-disconnected

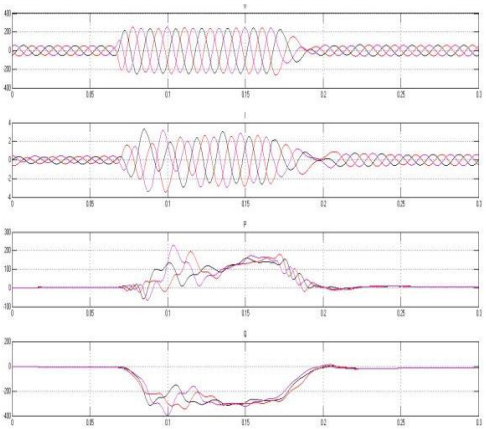

Figure 18: Result of Primary voltage, current, active power and reactive power

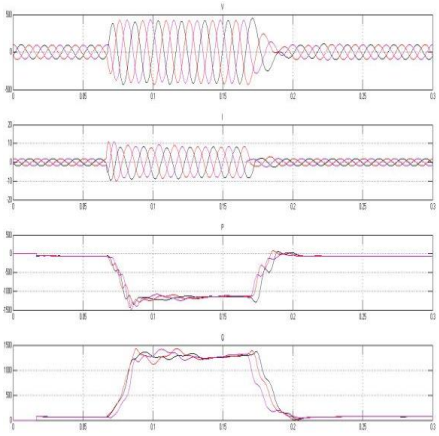

Figure 19: Result of Secondary voltage, current, active power and reactive power.

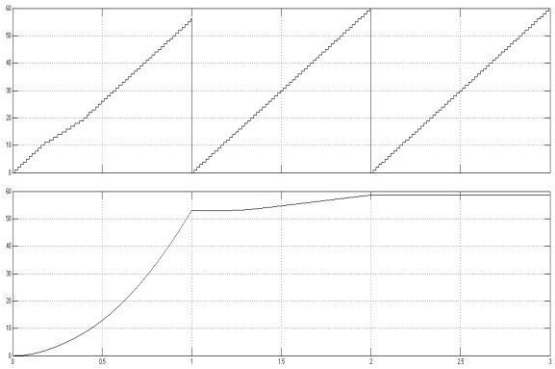

Figure 20 Result of Frequency

Case 5

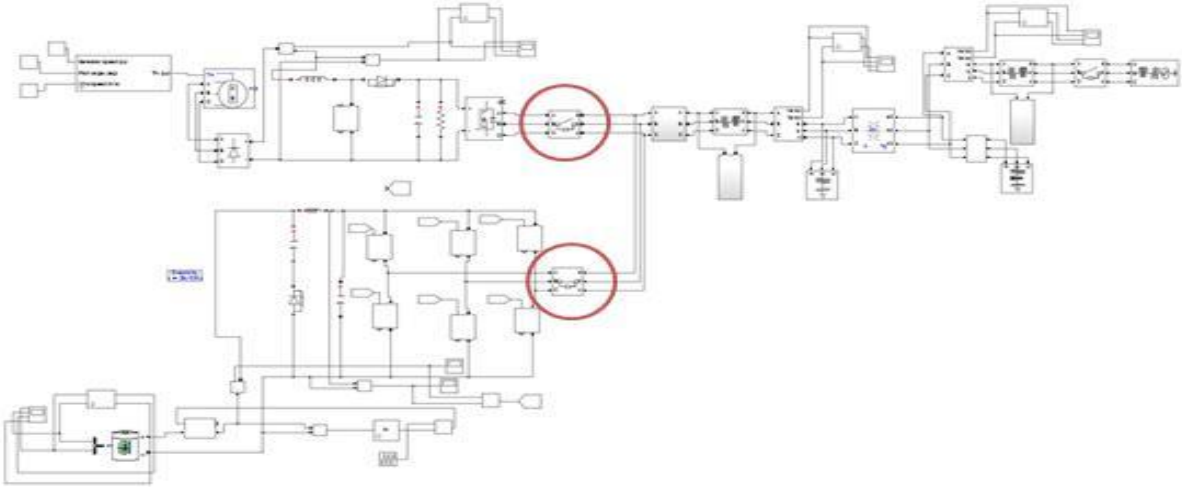

Figure 21: Battery supply in Grid-disconnected

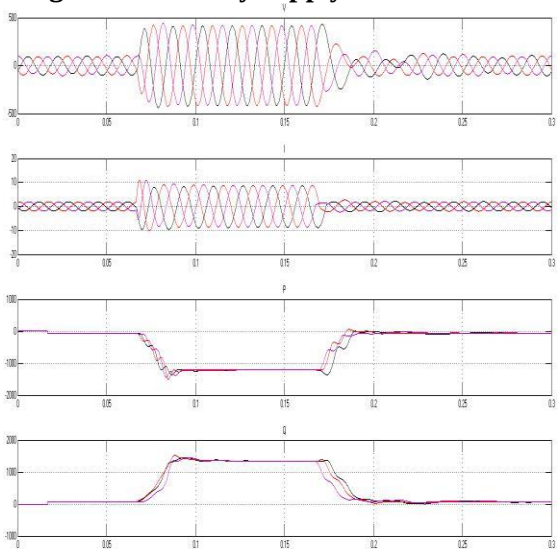

Figure 22: Result of Primary voltage, current, active power and reactive power

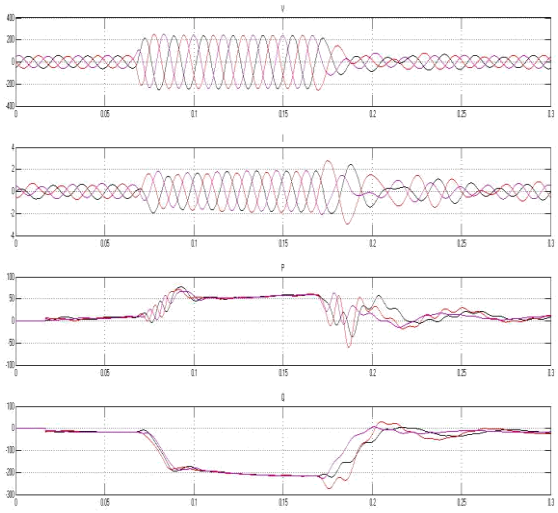

Figure 23: Result of Secondary voltage, current, active power and reactive power

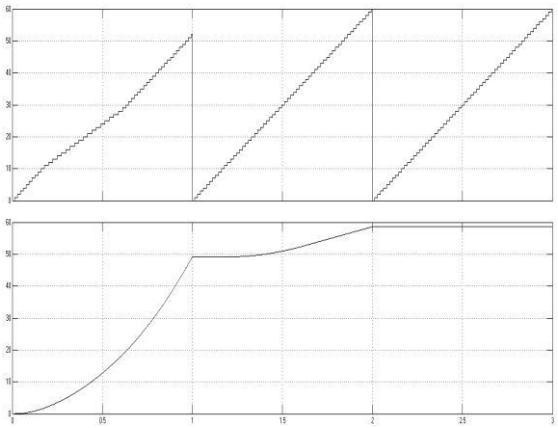

Figure 24 Result of Frequency

Case 6

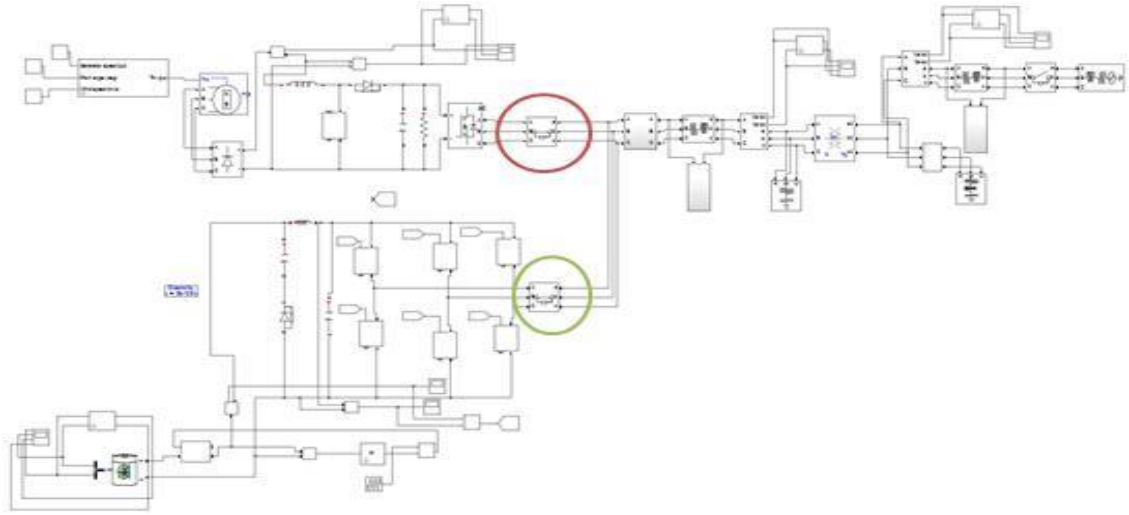

Figure 25: Wind turbine and Battery supply in Grid-disconnected

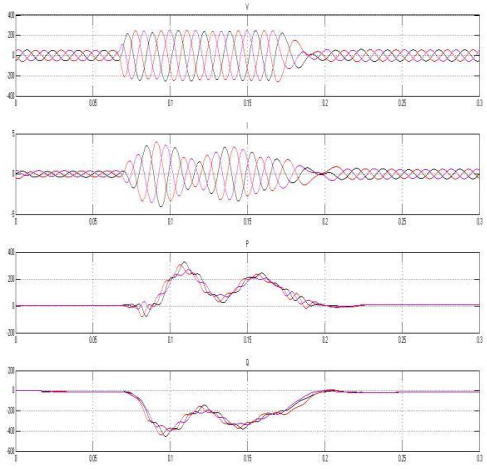

Figure 26: Result of Primary voltage, current, active power and reactive power

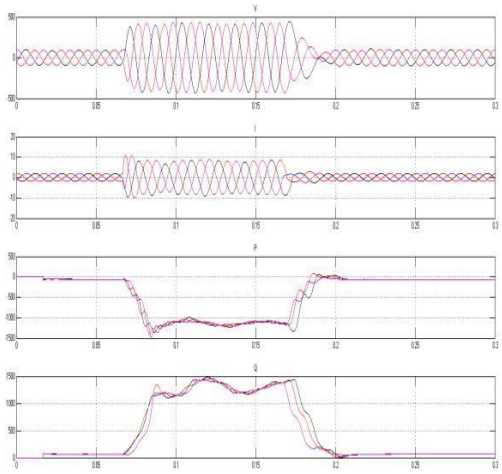

Figure 27: Result of Secondary voltage, current, active power and reactive power

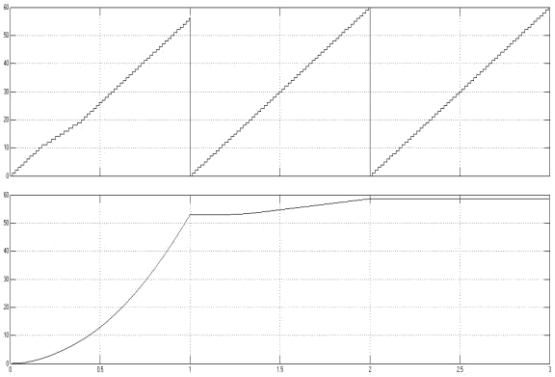

Figure 28 Result of Frequency

The time setting for all cases have transition time which is from 4/60 until 10/60 second at the breaker. It is means on that time the breaker will trigger from open to close and vice versa when it close to open. When the breaker in open condition, the current will flow through the snubber resistance inside of the breaker means the current can flow through at the resistance.

Table 1 Comparison Grid-connected and Grid-disconnected with Condition of Supply

WIND SUPPLY	BATTERY	PARAMETER	GRID-CONNECTED		GRID-DISCONNECTED	
			BEFORE	AFTER	BEFORE	AFTER
ON	OFF	VOLTAGE	240V	415V	54V	100V
		CURRENT	1.9A	8.5A	0.4A	1.9A
		ACTIVE POWER	60W	-1200W	7W	-60W
		REACTIVE POWER	-225Var	1300Var	-15Var	70Var
OFF	ON	VOLTAGE	240V	415V	55V	100V
		CURRENT	2.5A	8.5A	0.6A	2A
		ACTIVE POWER	150W	-1150W	9W	-80W
		REACTIVE POWER	-280Var	1300Var	-20Var	70Var
ON	ON	VOLTAGE	240V	415V	50V	90V
		CURRENT	1.9A	8.5A	0.4A	1.9A
		ACTIVE POWER	60W	-1200W	7W	-60W
		REACTIVE POWER	-225Var	1300Var	-15Var	70Var

Table 1 represent the value of voltage, current, active power and reactive power when the grid-connected and grid-disconnect with different condition of supply. Besides that, it shows before and after transformer that means before transformer represent the primary side of the transformer which is from supply and after transformer represent the secondary side of transformer which is from microgrid.

The value of voltage, current and reactive power when grid-connected is higher than when the grid-disconnected before and after transformer. The active power before transformer in grid-connected and grid-disconnected is positive that means the system cannot supply enough power to the load demand. The power output can be increased by adjust the value of load. For active power after transformer in grid-connected and grid-disconnected is negative that means the system have enough power to the load demand. So, the power load can be added or increase. The reactive power before transformer in grid-connected and grid-disconnected is negative means the reactive power flowing from grid to wind turbine and battery storage. For reactive power after transformer in grid-connected and grid-disconnected is positive means that reactive power is flowing from the wind turbine and battery storage to grid.

Frequency for both of grid-connected and grid-disconnected either before or after transformer gets the same value which is 60Hz. The value must same because the synchronization process need before connected to microgrid.

Grid-connected and Grid-disconnected at 11kV

Based on figure 4, shows the design to analyse the voltage, current, active power and reactive after connected to high voltage are 11kV. The 415V are step up by transformer to 11kV. The result was taken for this part at 415V side and 11kV side. There have two conditions which are grid-connected and grid-disconnected. The breaker use to close and open the circuit means when breaker is close, it show the grid is connected and when the breaker is open, it show the grid is disconnected. The reading of frequency also was taken at 415V side and 11kV side.

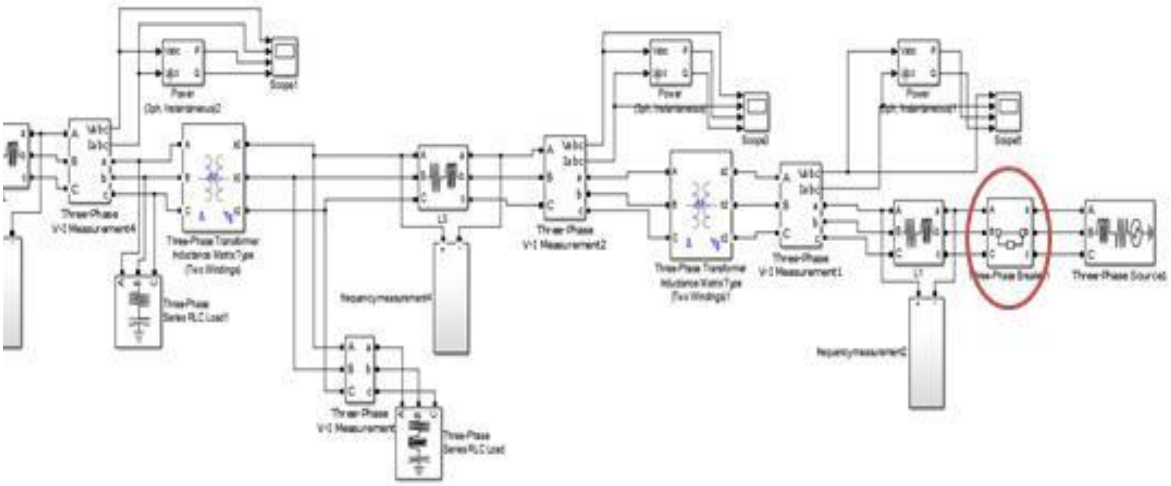

Figure 29: Design of 11kV in grid-connected

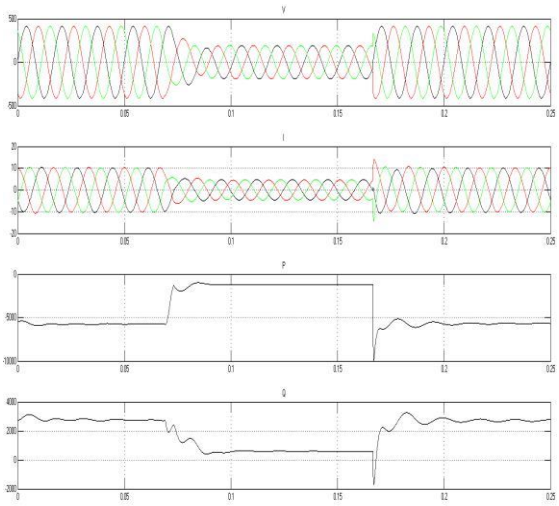

Figure 30: Result of Voltage, Current, Active Power and Reactive Power at primary side in grid-connected

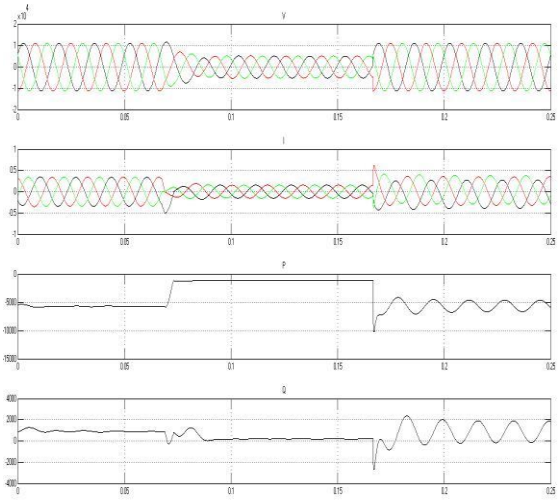

Figure 31: Result of Voltage, Current, Active Power and Reactive Power at secondary side in grid-connected

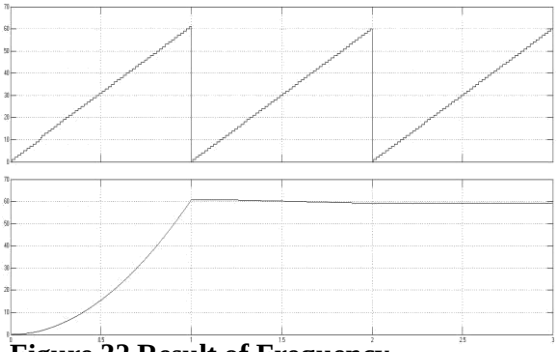

Figure 32 Result of Frequency

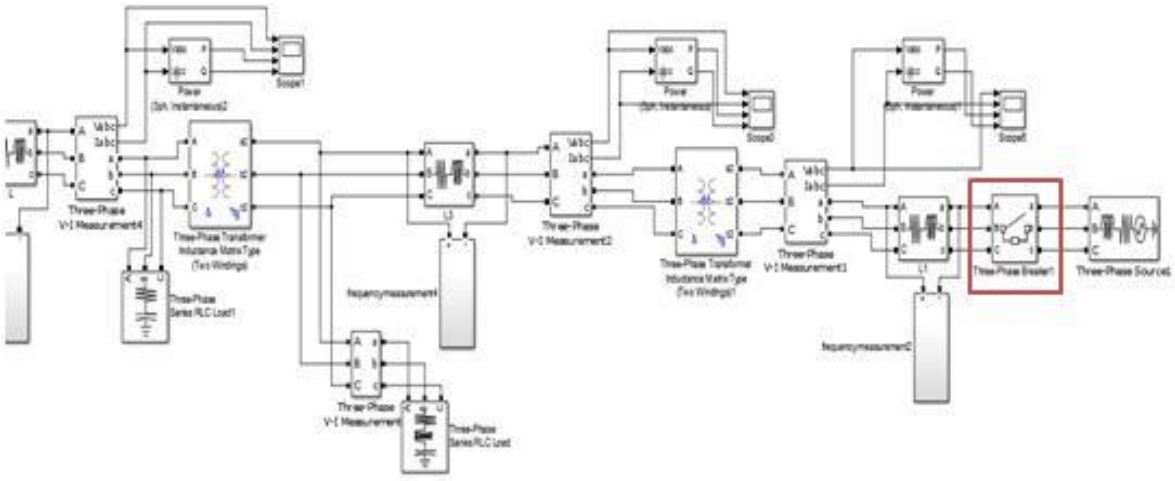

Figure 33: Design of 11kV in grid-disconnected

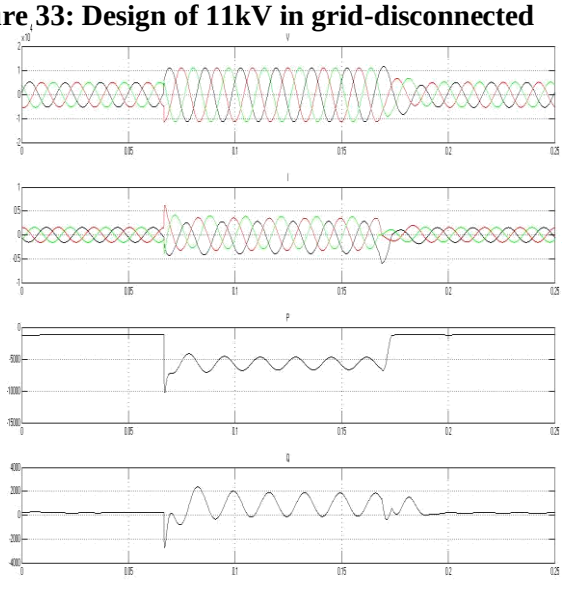

Figure 34: Result of Voltage, Current, Active Power and Reactive Power at

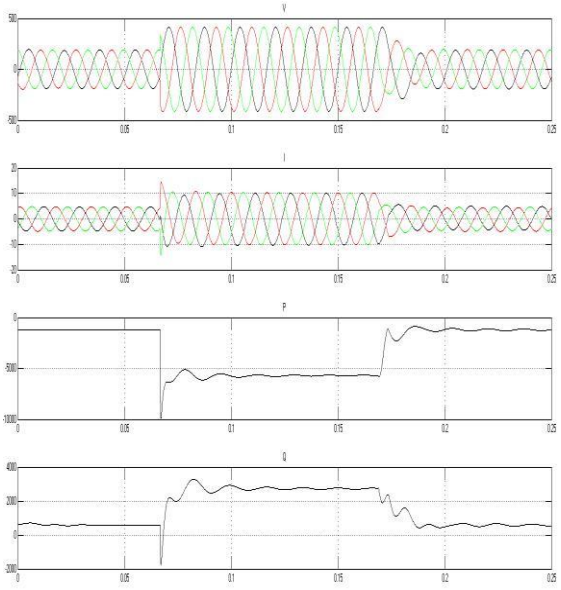

Figure 35: Result of Voltage, Current, Active Power and Reactive Power at

primary side in grid-disconnected **secondary side in grid-disconnected**

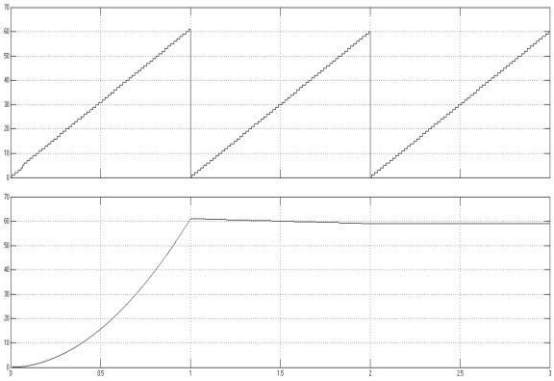

Figure 36 Result of Frequency

The time setting for all cases have transition time which is from 4/60 until 10/60 second at the breaker. It is means on that time the breaker will trigger from open to close and vice versa when it close to open. When the breaker in open condition, the current will flow through the snubber resistance inside of the breaker means the current can flow through at the resistance.

Table 2 Comparison of Grid-connected and Grid-disconnected of 11kV

Distribution system	Parameter	Grid-connected	Grid-disconnected
415 V	Voltage	415 V	200 V
	Current	10 A	4.7 A
	Active Power	-5600 W	-1200 W
	Reactive power	2800 Var	550 Var
11 kV	Voltage	11 kV	5.2 kV
	Current	0.35 A	0.15 A
	Active Power	-6700 W	-1200 W
	Reactive Power	1900 Var	200 Var

Table 2 represent the comparison between grid-connected and grid-disconnected at 11kV. The reading at grid-connected is higher than grid-disconnected. The voltage at 415V when grid-disconnected is 200V and the voltage at 11kV when grid-disconnected is 5.2kV. The current at 415V in grid-connected is 10A higher than in grid-disconnected is 4.7A. The current at 11kV also decrease from 0.35A in grid-connected to 0.15A in grid-disconnected.

The active power at 415V side in grid-connected is -5600W because have supply from grid. The active power at 415V in grid-disconnected increase to - 1200W because there do not get supply from the grid. The active power at 11kV side in grid-connected is -6700W because have supply from grid. The active power at 11kV in grid-disconnected increase to - 1200W because there do not get supply from the grid. The active power for both distribution 415V side and 11kV side are negative. Negative means the system have enough power to the load demand. So, the power load can be added or increase until the active power become 0. If the active power becomes positive means it not has enough supply.

The reactive power at 415V side in grid-connected is 2800Var higher than in grid-disconnected is 550Var. The reactive power at 11kV side in grid-connected is 1900Var higher than in grid-disconnected is 200Var. The reactive power at 415V side and 11kV side get the positive value. It is means that reactive power is flowing from the wind turbine and battery storage to grid

Conclusion

In conclusion, the model of wind turbine with battery storage connect to microgrid and load using MATLAB Simulink software are designed. The designs were made based on past research that have done before this. The design has wind turbine, rectifier, inverter, battery storage, breaker, load, transformer and grid. The performances of wind turbine with battery storage system connect to microgrid and load by using MATLAB Simulink Software are being analysed. The part has been analysed are voltage, current, active power and reactive power of the supply and grid. There have condition are being analysed. The performance of grid-connected and grid-disconnected by using MATLAB Simulink software are being analysed. The grid is step up from 415V before this to 11kV. The voltage, current, active power and reactive power were taken make comparison between grid-connected and grid-disconnected. So, the grid-connected performance had higher than grid-disconnected because the loads get the enough supply from supply and grid compared to grid-disconnected.

Acknowledgement

We wish to express our gratitude to honorable university, Universiti Teknikal Malaysia Melaka (UTeM). Special appreciation and gratitude to especially for Underwater Technology Research Group (UTeRG), Centre of Research and Innovation Management (CRIM), Center for Robotics and Industrial Automation (CERIA) for supporting this research and to Faculty of Electrical Engineering from UTeM for supporting this research under short term grand (PJP/2018/FKE(4C)/S01605).

References

[1] Lund H. Renewable energy strategiesforsustainable development. Energy 2007; 32:912–9.
[2] P. M. Anderson and A. Bose,“Stability simulation of wind turbine systems,” IEEE Trans.Power Appl. Syst., vol. PAS-102, no. 12, pp. 3791–3795, Dec. 1983.
[3] O. Ozgener,“A small wind turbine system (SWTS) application and its performance analysis”, EnergyConvers. Manag., vol. 47, pp. 1326–1337, Jul. 2006.
[4]Z. Lubosny; Wind Turbine Operation in Electric Power Systems; Springer-Verlag Berlin, 2002.
[5] N. Mohan, Advanced electric drives, MNPERE, 2001.
[6] R.W. Erickson; Fundamentals of Power Electronics, Kulwar Academic Publishers, 1997
[7] Yuhua Cheng; Chenming Hu (1999). "§2.1MOSFET classification and operation". MOSFET modeling & BSIM3 user's guide. Springer. p. 13. ISBN 0-7923-8575-6.
[8] Feltes James, Ralph Hendriks, Steven Stapleton, Ronald Voelzke, Baldwin Lam and Nancy Pfuntner. 2012. Twixt Land and Sea. Cost-Effective Grid Integration of Offshore Wind Plants. Volume10, Issue 2. Asia. IEEE power and energy magazine.
[9]Stauffer Nancy. 2006. Deep-sea oil rigs inspire MIT designs for giant wind tur-bines. Laboratory for Energy and the Environment.National Renewable Energy Laboratory. Accessed 22.09.2012

[10] Casanyi Edward; "Wind Energy End-Use Applications. EEP" - Electrical Engineering 2013.
[11]S. Chowdhury, S.P. Chowdhury, and P. Crossley. 2009. Microgrids and Active Distribution Newtwork. London: Institution of Engineering and Technology.

International Conference on Modern Applied Sciences, Engineering and Technology Application 2019 (ICMASET 2019)
eISBN: 978-967-2245-16-2
25th - 26th September 2019,
Bayview Beach Resort, Penang, Malaysia

TESTING of R-EMS 1.1 MODULAR RENEWABLE ENERGY MANAGEMENT SYSTEM WITH THE MINI SCADA CONCEPT USING IoT

Erik Tridianto[1]
Joke Pratilastiarso[2]
Prima Dewi P[3]
Muhammad Syafii WP[4]

[1] Mechanical And Energy Engineering Department, Politeknik Elektronika Negeri Surabaya (PENS), Indonesia, (E-mail: erik@pens.ac.id)
[2] Mechanical And Energy Engineering Department, Politeknik Elektronika Negeri Surabaya (PENS), Indonesia, (E-mail: joke@pens.ac.id)
[3] Mechanical And Energy Engineering Department, Politeknik Elektronika Negeri Surabaya (PENS), Indonesia, (E-mail: primadewi@pens.ac.id)
[4] Mechanical And Energy Engineering Department, Politeknik Elektronika Negeri Surabaya (PENS), Indonesia, (E-mail: syafiiw8@gmail.com)

Abstract: *The 4.0 industrial revolution marked by the existence of the Internet of Things caused the development of technology increasingly rapidly. That makes the need for the use of electrical energy also increases rapidly. Cooperation between the government and the community is needed to increase the role of renewable energy. Thus minimizing the use of electricity from PLN and optimizing electricity from renewable energy. Modular R-EMS is a technological innovation that enables the use of more than one renewable energy that can monitor and control wirelessly using the Internet of Things. Modular R-EMS has an interface to make the user easy to see the system. That Interface displays data in the form of voltage, current, power, percent of battery, monthly usage charge, and load back up system when PLN is not operating. Error generated at AC voltage 0.9% DC voltage 1.89% AC current 0.7% DC current 3%. In the process of sending data in the form of current and voltage from the module to the smartphone has a time lag of 3 seconds. The use of PLN energy at a load of up to 100% at night. The use of renewable energy in the morning 76.58% to 100% in the afternoon 78.95% - 100% in the afternoon 19.64% to 62.85%. The excess power from renewable energy automatically flows to PLN.*
Keywords: *Internet of Things, Modular R-EMS, Management Energy*

Introduction

The use of EBT (renewable energy) is being increased to reduce the use of non-renewable energy. The use of solar cells as electricity generation is still in the small and medium scale because solar cells utilize sunlight to produce electricity, this is a weakness of solar cells because when the daylight dims, solar panels will not produce electricity. So that PLN still has an important role in the supply of national electricity. In an effort to increase the national electrification ratio, it is necessary to collaborate between the community and the government that functions in enhancing the role of EBT, namely solar panels and wind turbines as environmentally friendly power plants. So that the government represented by PLN can increase the national electrification ratio to 100%. Studies show that around 9-18% of electricity savings can be achieved if users can obtain energy information directly [9].

Internet of Things or IoT is a communication technology innovation in the use of an expanded internet network that can be connected to other components and able to do monitoring and automatic control in real-time. With the availability of the internet network, the Internet of Things technology can be applied by identifying specifically the components of the objectives so that they can communicate online through the internet.

The Internet of Things technology that is developing at this time is an alternative in managing energy on electrical quantities such as current and voltage and performing automatic control of online relays.

Literature Review

Internet of Things

Kevin Ashton first conceived the Internet of Things in 1999, which allowed objects around to communicate through a network such as an internet. Starting from the Auto-ID center, technology based on radio frequency identification (RFID) which is the identification of electronic products that are unique and then developed into technology that every object can have an internet protocol (IP) address [5]. So IoT is a concept that forms a giant network that connects all devices to collect and share data about how a device is operated.

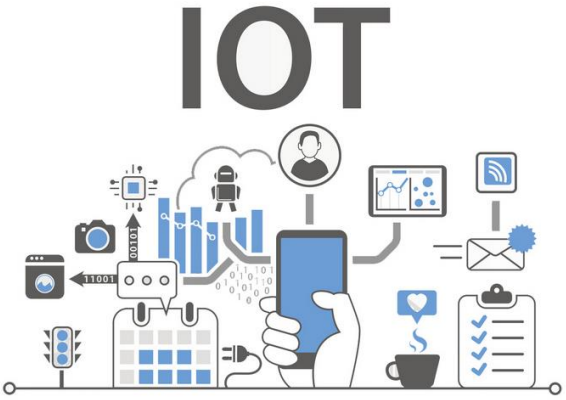

Figure 1: Internet of Things

Developments in the digital age have enabled technology to connect people with objects and also objects with objects. These supporting IoT technologies serve to illustrate how the various technologies relate to each other and communicate with each other with scalability, modularity, and configuration of IoT deployments in different scenarios.

SCADA

SCADA is an abbreviation of Supervisory Control and Data Acquisition, which serves to supervise, control, and process data in real-time in each process [7]. Real-time in a source stated, "real-time in a simple phrase is said that the user asks the computer system and then the computer system processes and answers it [4]. SCADA has four main parts, namely the Master terminal unit (MTU), Data communication, Remote terminal Unit (RTU), Field and Device.

MTU or master terminal unit is a system that functions as a server that receives data from RTU. Data from RTU is processed by MTU and displayed in the form of numbers and graphs according to the data that has been collected. MTU allows integration with HMI to make it easier to analyze data.

RTU or remote terminal unit is a system that is close to the object being observed. RTU is integrated with the sensor that is attached to the object being observed and functions as a

receiver of data from the sensor and sends data from the sensor to the MTU for data processing and analysis.

Communication is a system that connects RTU and MTU so that it can transmit data originating from sensors. SCADA performs data communication via radio, modem, optical fiber, and serial communication.

Field and Device are sensors and actuators that are attached to the observed object. The sensor functions to measure digitally and are received by RTU and sent to MTU for data analysis.

ON GRID PV SYSTEM

The grid-connected system is a system that is connected to a PLN cable so that it can sell the excess electricity available. This system uses solar panels (photovoltaic panels) to produce electricity that is environmentally friendly and emission-free. With this system will reduce household electricity bills, and provide added value to the owner. This series of systems will remain connected with the PLN network by optimizing the use of energy from solar panels to produce electrical energy as much as possible.

There are several studies that support this research. In that study, it is used as the basis for this research. Journal "Designing PLTS Hybrid Systems with PLN Electric Nets for Urban Homes." In the journal discusses the hybrid PLTS system with PLN, which uses batteries as a storage of electrical energy (storage system). The hybrid PLTS system with PLN electricity can be applied to urban homes, as well as analyzing factors that influence the amount of electrical energy produced by solar cells related to the working time of the PLTS system. PLTS will supply about 30% of electricity from the overall burden of household electrical equipment, while the remaining 70% of power is from PLN. (Bien, L E. 2008).

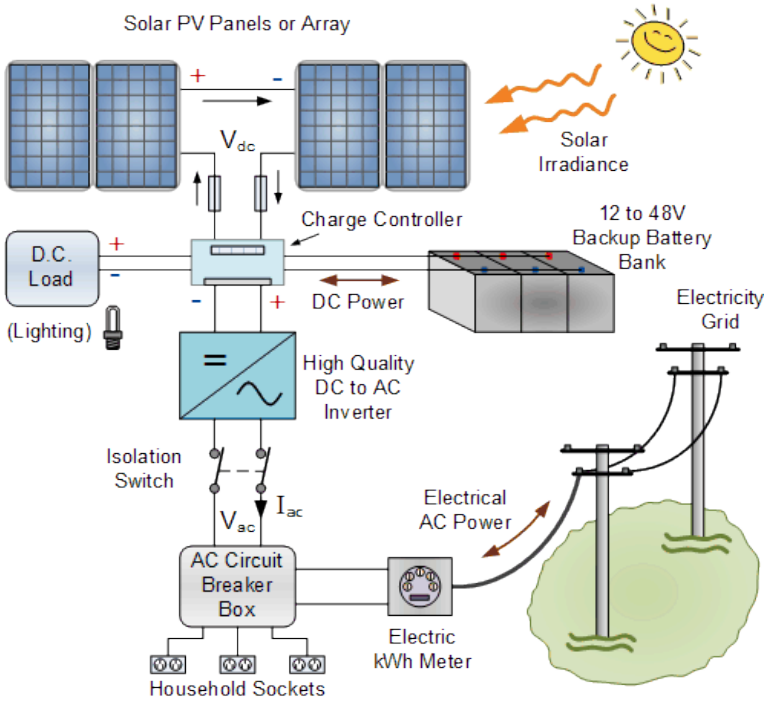

Figure 2: On Grid PV System

Comparative Study 2 Model of Power Plants Hybrid PLTS and PLN / Genset systems. In this journal discusses the comparison between PLTS model 1, which is hybrid with PLN and

PLTS model 2, which is made in series which is analyzed to get the best PLTS model. There are differences between the two models, namely the switch controller (PLTS regulator unit). Model 2 energy generated from PLTS, Genset, and windmills will be distributed directly to the battery and the load without any supply from PLN. From the configuration of the hybrid system model 1 and model 2 (both series and parallel), it can be concluded that the performance of the two models in principle has the same reliability in maintaining the continuity of power supply to the load, but from the simplicity of the equipment system, the PLTS 1 model is simpler than PLTS 2 model, and when viewed from the readiness of PLTS in supplying power to the load, the PLTS 2 model is far better than the PLTS 1 model, whereas from the investment side the model 2 is far more expensive than Model 1. (Indrajaya, 2012).

Study of PLTS Utilization as an Additional Power Supply in the Hospitality Industry in Nusa Lembongan, Bali. This study discusses the planning of a hybrid solar power plant with PLN, where the solar power system that will be developed to supply electricity is planned at 30%. The PLTS power that will be generated to supply the planned hotel energy is 21.6 kWp, which will be produced from 144 panels with a capacity of 150 Wp. The cost of PLTS energy at the current price of solar panels is Rp.8500 / Kwh. Taking into account the decline in the price of solar panels by an average of 9% per year and the tendency of an increase in world oil prices, it was found that in the next five years the PLTS energy costs would decrease to Rp.6100 / Kwh, close to the energy costs of a PLTD. The feasibility analysis of PLTS investment conducted using NPV, PI, and DPP shows the results that the PLTS investment is feasible to be carried out. Alternative strategies to determine the feasibility of PV-VP as an additional power supply are obtained by analyzing technical aspects, cost aspects, and regulatory aspects using a SWOT analysis. An alternative strategy from the SWOT analysis shows that the stipulation of regulations from the government is very instrumental in making the use of PLTS as an additional power supply, feasible to be developed in the hospitality industry in Nusa Lembongan, especially at the Bali Hai Tide Huts hotel. (Santiari, Dewa Ayu Sri 2011)

Modular Renewable Energy Management System

Modular Renewable Energy Management System (Modular R-EMS) adalah alat yang bisa melakukan monitoring, kontrol, serta proses management dari sumber renewable energi. Modular R-EMS terhubung secara wireless antar modulnya melalui internet yang kemudian terhubung pada cloud sehingga dapat dikontrol dan setiap datanya dapat diakses dimanapun melalui smartphone.

A. Modular R-EMS

Modular R-EMS has two main parts, namely hardware integrated with the concept of mini-SCADA and internet of things.

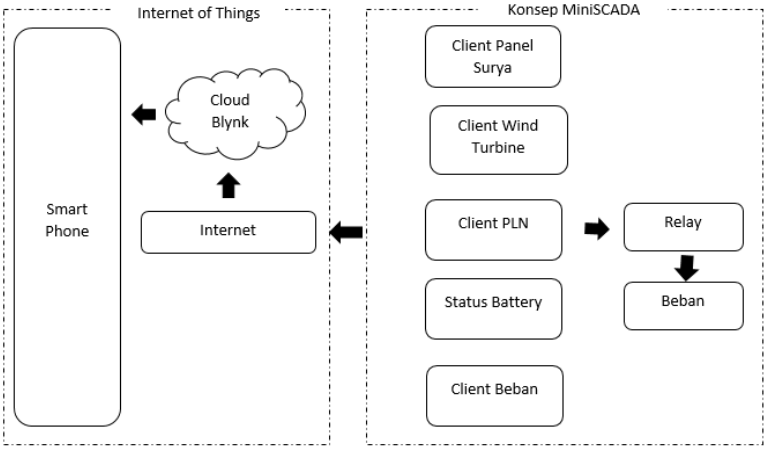

Figure 3: Diagram Block of R-EMS System

Integrated hardware with the Miniscada concept in this study consists of five R-EMS modules, each of which is mounted on a solar panel, wind turbine, PLN, Battery, and house load. In one of the R-EMS modules, there is a relay to control the source that we want to use. Internet of things consists of cloud and software embedded on smartphones.

B. Hardware Modular R-EMS

The R-EMS modular hardware is equipped with a voltage and current sensor to read the required quantities, and fitted with a relay to make the selection of the desired source. Sensors and relays are connected to Arduino and MCU nodes and then sent to the cloud via the internet.

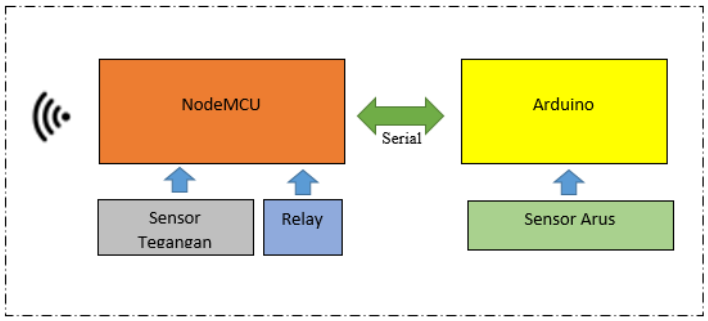

Figure 4: Diagram Block of R-EMS Hardware Design

C. Software Modular R-EMS

Software that is programmed on the Modular R-EMS is found on smartphones, either based on Android or IOS. From the application, the user can monitor the voltage, current, and power from the PLN, the load, the installed Renewable Energy, or the battery. And it is possible to see the costs that must be paid to PLN.

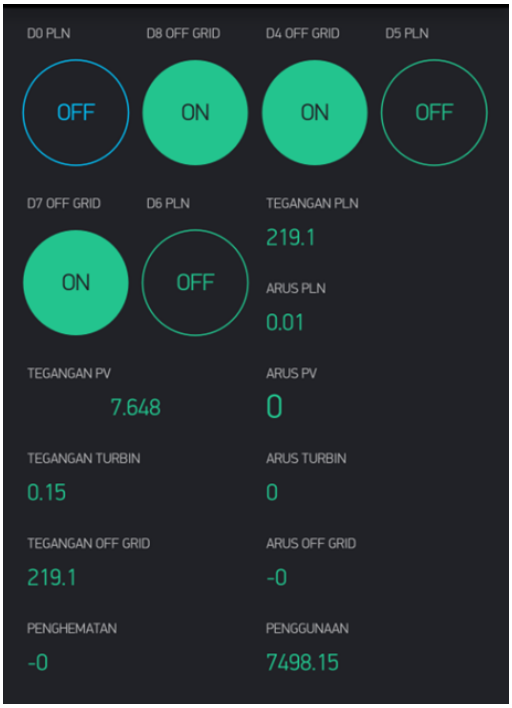

Figure 5: R-EMS Interface on Smartphones

Result And Analysis

After the modular R-EMS tool is finished, testing is needed to see its performance. Initially calibrated from each sensor installed. After the sensor calibration is complete the system testing of each R-EMS module is done to coordinate and carry out the process following what has been programmed

A. Testing of data transmission

Figure 6: Client Data Graph on the Server

In conducting microcontroller, communication requires the media to transmit analog and digital data. When communicating between two or more microcontrollers, serial

communication and wireless communication are used. Serial communication is used to send data in the form of numerical data in bytes to do data parsing on the destination microcontroller so that the data obtained by the data obtained can be executed with mathematical operations. In the process of sending data wirelessly, it takes communication media in the form of an internet network.

In the process of data communication from current sensors and voltage sensors needed In the process of sending data from the microcontroller, the transmitter needs the media to communicate. The media used in conducting wireless communication is by utilizing internet facilities obtained from smartphones connected to Wifi and data packages. When the smartphone is connected, the smartphone is ready to receive data from the client. The microcontroller that has been connected to the internet will upload data obtained from the conversion of the output signal from the current and voltage sensors. In the process of monitoring and control, the battery indicator needs to be considered to facilitate the selection of sources.

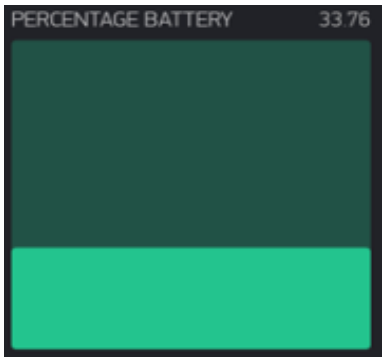

Figure 7: Battery Interface on Smartphones

B. R-EMS Modular Testing

System testing is done by taking data with variations in the load carried out at different times in the same place.

The first test was conducted on July 4, 2019, at 19:00 WIB.

Table 1: Hasil pengujian EBT On Grid pukul 19.00WIB

PLN		EBT		Beban	
Voltage (V)	Current (A)	Voltage (V)	Current (A)	Voltage (V)	Current (A)
223	0	223	0	223	0
223	0.42	223	0	223	0.41
223	0.75	223	0	223	0.73
223	0.99	223	0	223	0.96
223	1.14	223	0	223	1.08

In the first test, it was found that all the burden was borne by PLN; this is because, at night, the EBT / Solar panel could not produce electricity. It can be seen that the current generated by EBT is always 0 Amperes despite the change in load

The second test was conducted on July 5, 2019, at 15:30 WIB.

Table 2: Hasil pengujian EBT On Grid pukul 15.30WIB

PLN		EBT		Beban	
Voltage (V)	Current (A)	Voltage (V)	Current (A)	Voltage (V)	Current (A)
219	0.22	219	0.22	219	0
219	0.24	219	0.22	219	0.35
219	0.39	219	0.22	219	0.73
219	0.72	219	0.22	219	0.93
219	1.08	219	0.22	219	1.12

In the second test, the EBT power is 48.18 Watt, or in other words, the current generated is 0.22 Ampere. When testing with five different loads from 0.35 to 1.12 Amperes, data obtained that the R-EMS was successful in reading and displaying the configuration of the generated power. If EBT is higher, then EBT will send the remaining energy to PLN. And if the burden is higher than EBT, then the lack of power is obtained from PLN

The third test was conducted on July 6, 2019, at 11:30 WIB.

Table 3 : Hasil pengujian EBT On Grid pukul 11.30 WIB

PLN		EBT		Beban	
Voltage (V)	Current (A)	Voltage (V)	Current (A)	Voltage (V)	Current (A)
222	0.9	222	0.9	222	0
222	0.55	222	0.9	222	0.37
222	0.4	222	0.9	222	0.75
222	0.4	222	0.9	222	0.97
222	0.4	222	0.9	222	1.14

In the first variation which is conditioned to have no load, the on-grid inverter current is the same as the PLN current, and this is possible because the power generated by the On-grid inverter is excessive so that it is given to PLN for the amount of power generated. In the second and third variations, a load of 0.37 A and 0.75 A is needed because this is to know the power conditions of the EBT, PLN, and load. The results obtained in the second and third variations are that the load is still supplied by EBT because the power generated by EBT is greater than the load and the remainder of the power used for the load is given to PLN. In the fourth and fifth variations, it is known that EBT is not able to supply the power needed by the load so that power is needed from PLN.

Tests carried out using EBT load and power variations. Load variations are given to determine the magnitude of the comparison that occurs between the use of PLN and EBT. In tests conducted on July 4, 2019, at 19:00 IWST it is known that EBT does not produce current because the voltage needed to operate the On Grid inverter is not met. So that 100% power usage is supplied from PLN to the load.

Tests carried out on July 5, 2019 at 15:30 WIB it is known that the use of EBT at a load of 76.65 Watt at 62.85% and the use of PLN at 31.15% this is because the power supply from EBT has not been sufficient to meet the load requirements. Furthermore, an additional load of 159.87 Watt is carried out, with the power produced by EBT, which is relatively the same, the use of EBT is 30.13%, and PLN is 69.87%. At 203.67 Watt load usage, use EBT 23.66% and PLN 76.34% and 245.28 Watt load use EBT 19.64% and PLN 80.36%. The use of EBT continues to decrease while the use of load continues to increase. This is because the power

generated by EBT is not able to supply all the power needed by the load. So that PLN automatically adds less power than EBT to operate the load.

Tests conducted on July 6, 2019, at 11:30 IWST are known to produce the greatest power compared to previous tests so that the use of PLN is only 7-11%.

Conclusion

From the results and analysis of the research that has been done so that it can be concluded as follows:

1. The error obtained from testing the AC / DC voltage and current sensor compared to the measurement on the multimeter is less than 5%.
2. NodeMCU can be used as a microcontroller that can process data and upload data obtained from AC / DC voltage and current sensors in realtime and online.
3. In testing 1, the load consumption of PLN was 100%. Testing 2 load consumption of PLN worth 31% - 80%. Testing 3 load consumption of PLN is worth 12% - 23%. Testing 4 load consumption of PLN is worth 7% - 11%.

References

[1] Aditomo Syahrizal, Iwan Sugihartono, Muhammad Abdul Hadi, " Rancang Bangun Prototype Sistem Kontrol dan Monitoring Perangkat Listrik Rumah Tangga Berbasis Aplikasi Mobile Phone & Komputasi Awan (Cloud Computing)", Jatinagor, ISSN : 2477-0477.

[2] Aufa Al Anamila Nur, Teguh Yuwono, “Optimalisasi HMI SCADA untuk monitoring dan kontrol repeater radio komunikasi menggunakan modem GPRS intex J65i-X”,Gema teknologi ,Vol. 18 No.1, April – Oktober 2014.

[3] “ESP8266 802.11bgn Smart Device,” Espressif Systems. Datasheet.

[4] Fitriandi Afrizal, Endah Komalasari, Herri Gusmedi, " Rancang Bangun Alat Monitoring Arus dan Tegangan Berbasis Mikrokontroller dengan SMS Gateway ", Jurnal Rekayasa dan Teknologi Elektro, Vol.10 No.2 Mei 2016.

[5] Putra I Gusti Putu MastawanEka, Ida Ayu Dwi Giriantari, Lie jasa, " Monitoring Menggunaan Daya Listrik Sebagai Implementasi Internet of Things Berbasis Wireless Sensor Network ",Teknologi Elektro, Vol.16 No.3, September - Desember.

[6] Hudan Ivan Safril, Tri Rijanto, “Rancang bangun sistem monitoring daya listrik pada kamar kos berbasis Internet of Things (IoT)”,Surabaya,Vol.08 No.01 91-99,2019.

[7] Rahmawati putriana(2016),“ Rancang Bangun Mini SCADA Mikrokontroler Pada Renewable Energy Management System (R-EMS) ” , Politekhnik Elektronika Negeri Surabaya,Surabaya.

[8] Shobrina Upik Jamil, Rakhmadhany Primananda, Rizal Maulana, " Analisis Kinerja Pengiriman Data Modul Transceiver NRF24L01, Xbee dan Wifi ESP8266 Pada Wireless Sensor Network ", Jurnal Pengembangan Teknologi Informasi dan Ilmu Komputer,Vol.2 No.4, hlm.1510-1517

[9] C.H.Lien,”Remotely Controllable Outlet System for Home Power Management”, in tenth International Symposium on Consumer Electronics,Petersburg,2006.

[10]. H. Yuliansyah, "Uji Kinerja Pengiriman Data Secara Wireless Menggunakan Modul ESP8266 Berbasis Rest Architecture," Jurnal Rekayasa dan Teknologi Elektro, vol. 10, 2016.

[11]. E. Tridianto, P.D Permatasari, I.R Ali, "Experimental study of mini SCADA renewable energi management system on microgrid using Raspberry Pi," Journal of Physics, Conf. Series 983. IOP, 2017.

[12]. E. Tridianto, T.R Widcaksono "Maximum Power Point Tracking dengan Algoritma Perturb dan Observation untuk Turbin Angin," Jurnal Ilmiah SETRUM, vol. 5, 2016.

[13]. C. Hilman, E Tridianto, T.H Ariwibowo, Budiman P.A. Rohman, "Forecasting of Power Output of 2-Axis Solar Tracked PV Systems using Ensemble Neural Network," International Electronics Symposium on Engineering Technology and Applications (IES-ETA), 2017.

[14]. Budiman P.A. Rohman, C. Hilman, E Tridianto, T.H Ariwibowo Power Generation Forecasting of Dual-Axis Solar Tracked PV System Based on Averaging and Simple Weighting Ensemble Neural Networks," International Electronics Symposium on Engineering Technology and Applications (IES-ETA), 2017.

[15]. A.G, Safitra., F.H Sholihah, E Tridianto, C. Hilman, T.H Ariwibowo,I Baihaki Power Generation Forecasting of Dual-Axis Solar Tracked PV System Based on Averaging and Simple Weighting Ensemble Neural Networks," International Electronics Symposium on Engineering Technology and Applications (IES-ETA), 2017.

INTERNATIONAL CONFERENCE ON MODERN APPLIED SCIENCES, ENGINEERING AND TECHNOLOGY APPLICATION 2019 (ICMASET 2019)

ORGANIZING COMMITTEE:

Chairman:
Dr. Wan Azani Mustafa

Treasurer:
Zafira Zainudin

Technical Committee:
Nuratikah Amid Dudin

Technical Reviewer:
Dr Mohd Al Hafiz Mohd Nawi
Dr Nurul Ain Chua Binti Abdullah
Ir. Dr Mohd Farriz Bin Hj Basar
Dr. Harwati Hashim
Ts ChM Dr Khalisanni Khalid
Dr. Ahmad Shidki b. Mat Yusoff
Fahmi Zaidi Bin Abdul Razak
Dr Fan Siong Peng

Liaison Officer:
Nur Hajar Binti Mohamad Fadzil

Published by:
Global Academic Excellence (M) Sdn. Bhd.
(1257579-U)
KELANTAN, MALAYSIA

eISBN 978-967-2245-16-2